

Discovery of AM-7209, a Potent and Selective 4-Amidobenzoic Acid Inhibitor of the MDM2–p53 Interaction

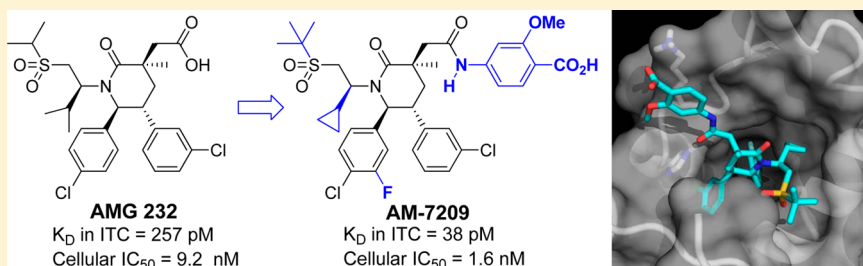
Yosup Rew,^{*,†} Daqing Sun,[†] Xuelei Yan,[†] Hilary P. Beck,[†] Jude Canon,^{||} Ada Chen,[†] Jason Duquette,[†] John Eksterowicz,[†] Brian M. Fox,[†] Jiasheng Fu,[†] Ana Z. Gonzalez,[†] Jonathan Houze,[†] Xin Huang,[⊥] Min Jiang,[§] Lixia Jin,[§] Yihong Li,[†] Zhihong Li,[†] Yun Ling,[§] Mei-Chu Lo,[†] Alexander M. Long,[⊥] Lawrence R. McGee,[†] Joel McIntosh,[†] Jonathan D. Oliner,^{||} Tao Osgood,^{||} Anne Y. Saiki,^{||} Paul Shaffer,[⊥] Yu Chung Wang,^{||} Sarah Wortman,[‡] Peter Yakowec,[⊥] Qiuping Ye,[§] Dongyin Yu,^{||} Xiaoning Zhao,[†] Jing Zhou,[†] Julio C. Medina,[†] and Steven H. Olson[†]

[†]Department of Therapeutic Discovery, [‡]Department of Pharmaceutics, and [§]Department of Pharmacokinetics and Drug Metabolism, Amgen Inc., 1120 Veterans Boulevard, South San Francisco, California 94080, United States

^{||}Department of Oncology Research, Amgen Inc., One Amgen Center Drive, Thousand Oaks, California 91320, United States

[⊥]Department of Therapeutic Discovery, Amgen Inc., 360 Binney Street, Cambridge, Massachusetts 02142, United States

S Supporting Information



ABSTRACT: Structure-based rational design and extensive structure–activity relationship studies led to the discovery of AMG 232 (**1**), a potent piperidinone inhibitor of the MDM2–p53 association, which is currently being evaluated in human clinical trials for the treatment of cancer. Further modifications of **1**, including replacing the carboxylic acid with a 4-amidobenzoic acid, afforded AM-7209 (**25**), featuring improved potency (K_D from ITC competition was 38 pM, SJS-A1 EdU IC_{50} = 1.6 nM), remarkable pharmacokinetic properties, and in vivo antitumor activity in both the SJS-A1 osteosarcoma xenograft model (ED_{50} = 2.6 mg/kg QD) and the HCT-116 colorectal carcinoma xenograft model (ED_{50} = 10 mg/kg QD). In addition, **25** possesses distinct mechanisms of elimination compared to **1**.

INTRODUCTION

p53 is a short-lived transcription factor which plays a critical role in preventing tumor development. It is stabilized by cellular stress and accumulates in the nucleus. Activated p53 binds to DNA and increases transcription of numerous genes involved in cell cycle arrest, DNA repair, senescence, and apoptosis.^{1,2} Accordingly, loss of p53 function in tumor cells provides a strong selective growth advantage, and it has been proposed that dysfunction in the p53 pathway may be a required step in tumor development.³ Multiple independent studies have demonstrated that loss of p53 function contributes to tumor progression. Furthermore, restoring endogenous p53 function in established tumors results in tumor regression in vivo and could be an effective anticancer therapeutic approach.^{4–7}

The MDM2 (murine double minute 2) oncogene is a key cellular negative regulator of p53. MDM2 is transcriptionally activated by p53 and, in turn, inhibits p53 by controlling its activity,⁸ subcellular location,^{9–11} and degradation.^{12,13} Inhibi-

tion of the MDM2–p53 interaction with small-molecule MDM2 inhibitors has been shown to be a tractable strategy for reactivation of the p53 pathway in tumors with wild-type p53,^{14,15} which is present in approximately 50% of human cancers.¹⁶ The potential benefits of neutralizing the MDM2–p53 protein–protein interaction have been recognized for nearly 20 years, and recently, several small molecules interdicting the target have advanced into clinical trials.^{17–21}

We discovered AMG 232 (**1**) (Figure 1), a novel piperidinone inhibitor of the MDM2–p53 interaction via structure-based rational design using conformational control and extensive SAR studies.^{21–23} Herein, we report the continued investigation of **1**, which led to the discovery of AM-7209 (**25**), a novel 4-amidobenzoic acid-containing MDM2 inhibitor that possesses structural differentiation and distinct in vivo mechanisms of elimination compared to **1**.

Received: October 7, 2014

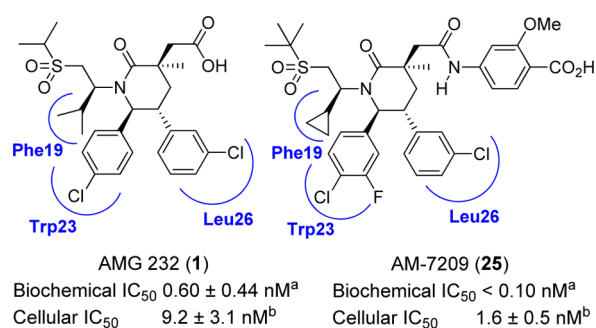


Figure 1. Chemical structures and potencies of **1** and **25**. MDM2 binding pockets are labeled (by p53 side chain) in blue. Notes: (a) IC₅₀ in the HTRF biochemical assay (serum free),²⁴ (b) IC₅₀ in the EdU cell proliferation assay (SJS-A-1, 10% human serum).²⁴

RESULTS AND DISCUSSION

As previously reported,^{21b} compound **2** (Table 1), the *tert*-butyl sulfone analogue having a cyclopropyl group at the α position of the *N*-alkyl group, was extremely potent due to the favorable interactions of the cyclopropyl group and the *tert*-butyl group with MDM2. However, **2** exhibited rapid turnover in human hepatocytes, resulting in a high projected clearance in humans. Adding fluorine to the C5 or C6 aryl group furnished even more potent *tert*-butyl sulfones **3** and **4**, but yielded no improvement of metabolic stability in human hepatocytes.

The crystal structure of the 109-residue amino-terminal domain of MDM2 bound to a 15-residue transactivation domain peptide of p53 disclosed that MDM2 has three hydrophobic clefts that bind three critical residues of p53 (Phe19, Trp23, and Leu26).²⁵ The binding modes of compounds **1–4** were predicted from the X-ray cocrystal structures of related analogues (Figure 2).^{21,22}

The C6 *p*-Cl-phenyl occupies the deepest Trp23_(p53) pocket, and the C5 *m*-Cl phenyl reaches into the Leu26_(p53) pocket. The latter interaction is augmented by a face-to-face π -stacking interaction with His96. The C3 methyl drives the *trans* C5 and C6 aryl groups to reside in a gauche-like orientation, the favored conformation for binding to MDM2. The isopropyl group (for **1**) or the cyclopropyl group (for **2–4**) at the α position of the *N*-alkyl group is forced into the Phe19_(p53) pocket by the conformational constraint induced by α -

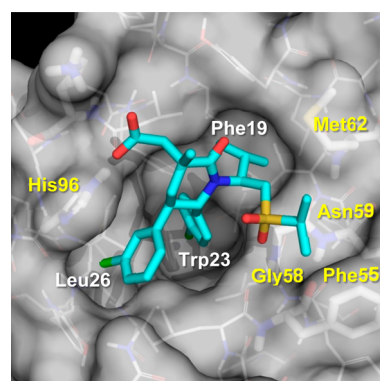


Figure 2. Binding mode of compound **1** based on the cocrystal structures of its analogues bound to human MDM2 (17–111).²¹ MDM2 binding pockets are labeled (by p53 side chain) in white. MDM2 residues Phe55, Gly58, Asn59, Met62, and His96 are labeled in yellow.

substitution. The isopropyl (for **1**) or *tert*-butyl (for **2–4**) moiety attached to the sulfonyl group lies in the “Gly58 shelf” region (Phe55, Gly58, Asn59, and Met62) and engages in a hydrophobic interaction with this region, while the sulfone function is close to the α -carbon of Gly58, inducing a CH \cdots O-type interaction with this residue. Lastly, the carboxylic acid is located on top of the His96 side chain of MDM2 and interacts with the adjacent, and presumably protonated, imidazole of His96.

Preliminary metabolite profiling studies indicated that compound **2** was mainly cleared through glucuronidation of the carboxylic acid in human hepatocytes (data not shown). Thus, we hypothesized that replacing the carboxylic acid with other functional groups to reduce glucuronidation but maintain an interaction with the imidazole of His96 in MDM2 could improve the metabolic stability of the cyclopropyl analogues (**2–4**) without diminishing their superb potency.

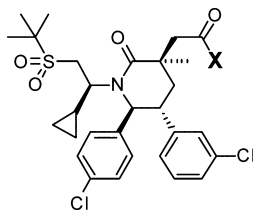
Our investigation started with the conversion of the carboxylic acid into amides (Table 2). Both primary amide **5** and phenyl amide **6** were well tolerated in the biochemical assay (**5** and **6** vs **2**), suggesting that an amide can also have a hydrogen bond interaction with the side chain of His96. This result was consistent with the previous findings in the X-ray

Table 1. Potent *tert*-Butyl Sulfone Derivatives

	1	2	3	4
biochemical potency				
IC ₅₀ ^a (HTRF) (nM)	0.63 ± 0.44	0.10 ± 0.01	0.10 ± 0.03	<0.10
cellular potency (SJS-A-1)				
p21 IC ₅₀ ^a (10% HS ^b) (nM)	47 ± 15	18.1 ± 4.2	15.5 ± 9.2	6.4 ± 3.5
EdU IC ₅₀ ^a (10% HS ^b) (nM)	9.2 ± 3.1	1.6 ± 0.8	1.2 ± 0.3	0.80 ± 0.25
human hepatocyte CL _{int} (μ L/min/10 ⁶ cells)	6.3	16	26	27

^aPotency data are reported as the mean and standard deviation of at least two determinations. ^bHS = human serum.

Table 2. Amidobenzoic Acid Derivatives



Compd	X	Biochemical Potency	Cellular Potency (SJS-1)
		HTRF IC ₅₀ ^a (nM)	EdU (10% HS ^b) IC ₅₀ ^a (nM)
2		0.10 ± 0.01	1.6 ± 0.8
5		0.17 ± 0.05	33 ± 9
6		0.37 ± 0.04	85 ± 18
7		0.18 ± 0.06	2.9 ± 0.6
8		0.13 ± 0.07	1.9 ± 0.5
9		0.18 ± 0.03	6.9 ± 0.9
10		0.21 ± 0.07	9.7 ± 0.8
11		0.37 ± 0.13	45 ± 11
12		0.49 ± 0.19	15 ± 1
13		2.4 ± 0.9	138 ± 21
14		0.21 ± 0.05	9.0 ± 2.8
15		0.21 ± 0.07	2.7 ± 0.2
16		1.8 ± 0.7	198 ± 119

^aPotency data are reported as the mean and standard deviation of at least two determinations. ^bHS = human serum.

cocrystal structures of the oxindole inhibitors with MDM2 by us²³ and others.¹⁹ However, amides 5 and 6 were significantly less potent than carboxylic acid 2 in the cell proliferation assay (20–50-fold), presumably due to the poor permeability. Extensive investigation on carboxylic acid replacements including various amide modifications was carried out to modulate the properties of the amide derivatives.²⁶ Interestingly, when an additional carboxylic acid moiety was introduced at the *para*-position of the phenyl group in 6, cellular potency

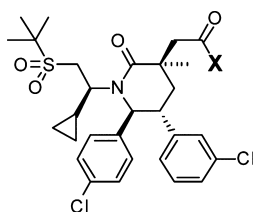
was significantly improved (7 vs 6) and compound 7 was almost equipotent with 2. Furthermore, compound 7 exhibited significantly enhanced stability in human hepatocytes [human hepatocyte CL_{int} (μL/min/10⁶ cells) = 3.2 for 7 vs 16 for 2, Table 4]. Recently, an approach has been reported where a *p*-benzoic acid side chain was added to pyrrolidine-derived MDM2 inhibitors to improve their pharmacokinetic (PK) parameters.¹⁹

Encouraged by the superior potency and improved metabolic stability of 7 in human hepatocytes, further investigation of the benzoic acid moiety was conducted (Table 2). Adding a methoxy group at the *ortho*-position was tolerated (8), but shifting it into the *meta*-position diminished the potency (9). Moving the amino group from the *para*-position to the *meta*- and *ortho*-positions reduced the potency, particularly in the cell proliferation assay (10 and 11 vs 7). Converting the carboxylic acid into a primary amide or a nitrile resulted in a significant reduction in potency (12 and 13). Changing the benzoic acid to a phenylacetic acid or replacing the phenyl ring with a pyridine ring was well tolerated (14 and 15), while *N*-methylation resulted in loss of potency (16).

Replacement of the phenyl ring between the acid and the amide nitrogen with a nonaromatic ring was also explored (Table 3). The *trans*-cyclohexanecarboxylic acid analogue 17 exhibited a slightly decreased activity in both the biochemical and cell proliferation assays compared to 7. The *cis* analogue 18 was even less potent in the cell proliferation assay. The potency of the bicyclo[2.2.2]octane analogue 19, which has a linear topology, was close to the potency of 7. The piperidinecarboxylic acid derivatives 20 and 21 exhibited potency comparable to that of the *trans*-cyclohexanecarboxylic acid analogue 17. Decreasing the ring size from a six-membered ring to a four-membered ring resulted in no potency improvement in biochemical or cell proliferation assays (17, 18, and 20 vs 22–24).

Adding a fluorine to the C5 or C6 aryl group of the piperidinone core in 8 provided two extremely potent compounds, 25 and 26, which were derived from 3 and 4, respectively (Table 4). The amide-containing compounds 7, 8, 19, 25, and 26 retained their potency in both biochemical and cell-based assays compared to the simple carboxylic acids 2–4 in Table 1. These compounds were further profiled for CYP inhibition, PXR activation, and CYP time-dependent inhibition (TDI). All were found to have minimal liabilities in these assays, and furthermore, the metabolic stability of these compounds in human hepatocytes was greatly improved [human hepatocyte CL_{int} (μL/min/10⁶ cells) = 1.5–4.6 for 7, 8, 19, 25, and 26 vs 16–27 for 2–4]. On the basis of PK profiles in dog, predicted human PK, and rodent toxicology studies (data not shown), 25 was selected for further evaluation.

The reported dissociation constant (*K*_D) of 1 was 45 pM in a surface plasmon resonance (SPR) spectroscopy binding assay,²¹ while 25 had a *K*_D that was too low to be determined under identical assay conditions. In an isothermal titration calorimetry (ITC) competition assay, the *K*_D for 25 and 1 was measured as 38 and 257 pM, respectively.²⁴ Compound 25 was consistently more potent than 1 in both the HTRF biochemical assay (IC₅₀ = <0.10 nM vs 0.60 nM) and the cell proliferation assay in the MDM2 amplified SJS-1 osteosarcoma cell line (IC₅₀ = 1.6 nM vs 9.2 nM). In addition to its significant *in vitro* potency, compound 25 showed pharmacokinetic properties both in mouse (iv CL = 0.026 L/h/kg, po *F* = 30%) and in dog (iv CL

Table 3. Replacement of the Phenyl Ring with a Nonaromatic Ring

Compd	X	Biochemical Potency	Cellular Potency (SJS-1)
		HTRF IC ₅₀ ^a (nM)	EdU (10% HS ^b) IC ₅₀ ^a (nM)
7		0.18 ± 0.06	2.9 ± 0.6
17		0.73 ± 0.35	7.5 ± 0.4
18		0.42 ± 0.24	17.0 ± 2.5
19		<0.10	5.9 ± 0.8
20		0.79 ± 0.25	11.7 ± 1.5
21		0.49 ± 0.15	6.8 ± 0.7
22		0.52 ± 0.22	13.5 ± 0.4
23		0.83 ± 0.35	22 ± 3
24		0.26 ± 0.18	46 ± 4

^aPotency data are reported as the mean and standard deviation of at least two determinations. ^bHS = human serum.

= 0.69 L/h/kg, po $F = 45\%$) (iv = intravenous, po = per os) sufficient to support further development.

The cocrystal structure of **25** with MDM2 (PDB code 4WT2) revealed that it binds to the protein in a manner consistent with the predicted binding mode of compound **1** (Figure 3). Notably, the amide oxygen of **25** interacts with the His96 imidazole in a manner analogous to that of the carboxylate of compound **1**. In addition, the cocrystal structure shows that the carboxylic acid in **25** and the amine of Lys94 are in close proximity, but solution NMR studies failed to provide evidence of an interaction.²⁷

To evaluate its selectivity, the effect of **25** on inhibiting the proliferation of HCT-116 p53^{wt} and p53^{-/-} tumor cells in vitro was examined (Figure 4).²⁴ In accordance with the data observed for **1** and other piperidinone analogues,^{21,22} **25** potently inhibited cell growth on-target in the tumor cell line with wild-type p53 cells (IC₅₀ = 2.0 nM) and exhibited more than 12500-fold selectivity over those with p53-deficient cells (off-target IC₅₀ > 25 μM).

An in vivo pharmacodynamic (PD) study²⁸ with **25** in an SJS-1 tumor xenograft mouse model showed a dose-dependent induction of p21 mRNA, a direct transcriptional marker of p53 activity.²⁹ This outcome clearly indicated an on-mechanism activation of the p53 pathway by **25** (Figure 5). A concentration-dependent peak induction of p21 mRNA was observed approximately 4 h after dosing (30-fold induction at 10 mg/kg and 10-fold induction at 3 mg/kg).

Next, compound **25** was evaluated for its ability to inhibit tumor growth in an SJS-1 mouse xenograft model.²⁸ Consistent with the findings of the PD study, robust dose-dependent tumor growth inhibition was observed. Compound **25** completely inhibited tumor growth at 10 mg/kg QD compared to vehicle with an ED₅₀ of 2.6 mg/kg (Figure 6). The calculated unbound EC₅₀ associated with the ED₅₀ was 2.0 nM.³⁰ Notably, both the 25 mg/kg QD dose and the 50 mg/kg QD dose of **25** caused complete tumor regression in 9 of 10 mice and 10 of 10 mice, respectively. Tumors in the 50 mg/kg group continued to show complete regression for 30 days after treatment (data not shown). There was no significant body weight loss or other signs of toxicity observed in any of the treatment groups (≤±5%).

Moreover, in the HCT-116 colorectal carcinoma mouse xenograft model, treatment with **25** caused a dose-dependent reduction in tumor growth with an ED₅₀ of 10 mg/kg. At a dose of 100 mg/kg QD, 100% tumor growth inhibition was observed (Figure 7).²⁸ There was also no body weight loss in any of the treatment groups. The effective inhibition of tumor growth in the p53^{wt} HCT-116 tumors with normal MDM2 expression confirmed that the neutralization of the MDM2–p53 interaction with a small-molecule MDM2 inhibitor could be an efficacious therapeutic strategy against tumors that are p53^{wt}.

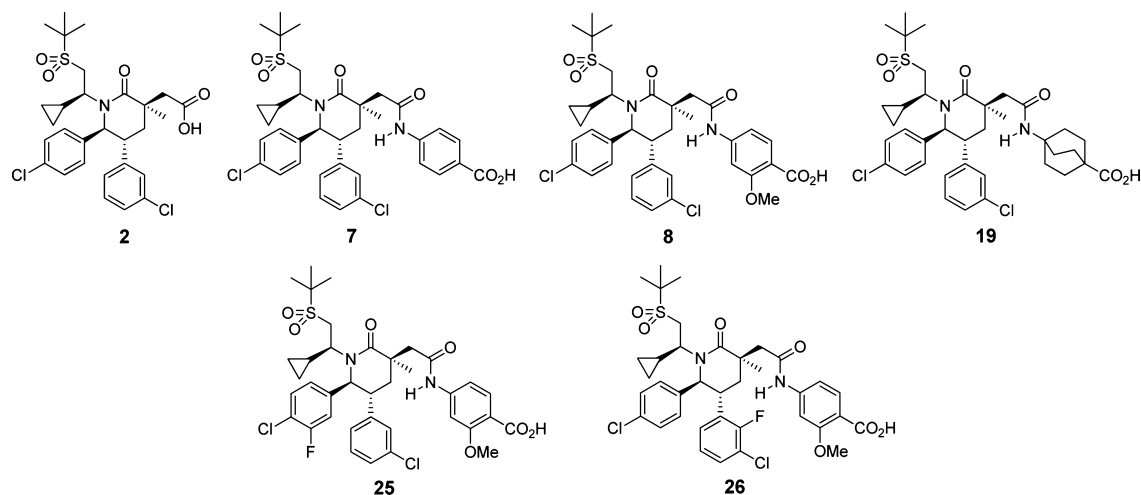
What clearly differentiated **25** from **1** was its different metabolic profile. When incubated in rat, dog, cyno, and human hepatocytes,³¹ compound **1** is converted exclusively to the acyl glucuronide (M1) (Figure 8a). In contrast, hepatocyte incubation of compound **25** provided oxidative metabolite M2 as the major product, although phenol M3, produced via oxidative demethylation, and acylglucuronide M1 were also detected (Figure 8b). The reported structural modifications alter the metabolic fate of the molecules, which was an important consideration for this backup program.

CHEMISTRY

The synthesis of target compounds started with the preparation of lactone intermediates **30a–30c**. The synthesis of **30a** was previously reported.³² Lactones **30b** and **30c** were prepared according to the procedures described for the synthesis of **30a**, replacing ketone **27a**^{21,32} with the appropriate ketones **27b** and **27c**, respectively (Scheme 1). Michael addition of **27b** and **27c** to methyl methacrylate provided δ -keto esters **28b** and **28c**, which were subjected to a dynamic kinetic resolution (DKR) using a Noyori catalyst. Following a two-step hydrolysis/lactonization sequence, lactones **29b** and **29c** were obtained as a mixture of epimers at C3 [er > 83:17 in favor of the (5*R*,6*R*)-isomer]. Diastereoselective allylation at C3 of *cis*-5,6-disubstituted δ -lactones **29b** and **29c** gave C3 quaternized lactones **30b** and **30c** with excellent selectivity (dr > 95:5). Recrystallization of the lactones **30b** and **30c** from DCM in hexanes easily improved the er to >99:1.

Compounds **2–4** were synthesized from lactones **30a–30c** utilizing the bicyclic iminium ether chemistry shown in Scheme

Table 4. Potent Amide-Containing Derivatives



	2	7	8	19	25	26
biochemical potency						
IC ₅₀ ^a (HTRF) (nM)	0.10 ± 0.01	0.18 ± 0.06	0.13 ± 0.07	<0.10	<0.10	<0.10
IC ₅₀ ^a (HTRF, 15% HS ^b) (nM)	1.1 ± 0.6	0.60 ± 0.03	0.50 ± 0.19	0.70 ± 0.14	0.60 ± 0.13	0.50 ± 0.22
cellular potency (SJS-1)						
p21 IC ₅₀ ^a (10% HS ^b) (nM)	18.1 ± 4.2	10.4 ± 2.8	13.9 ± 7.0	26.5 ± 4.7	13.7 ± 5.2	6.1 ± 2.0
EdU IC ₅₀ ^a (10% HS ^b) (nM)	1.6 ± 0.8	2.9 ± 0.6	1.9 ± 0.5	5.9 ± 0.8	1.6 ± 0.5	1.0 ± 0.2
CYP3A4 inhibition (%) at 3 μM	<10	<10	14	<10	<10	14
hPXR activation (%) compared to the control ^c at 2 μM	28	0	14	0	0	0
remaining activity (TDI) (%) of CYP3A4 compared to the control ^d after 30 min at 10 μM	75	78	85	75	63	72
human hepatocyte CL _{int} (μL/min/10 ⁶ cells)	16	3.2	4.6	3.7	1.5	1.7

^aPotency data are reported as the mean and standard deviation of at least two determinations. ^bHS = human serum. ^cRifampin used as a positive control. ^dDMSO used as the control.

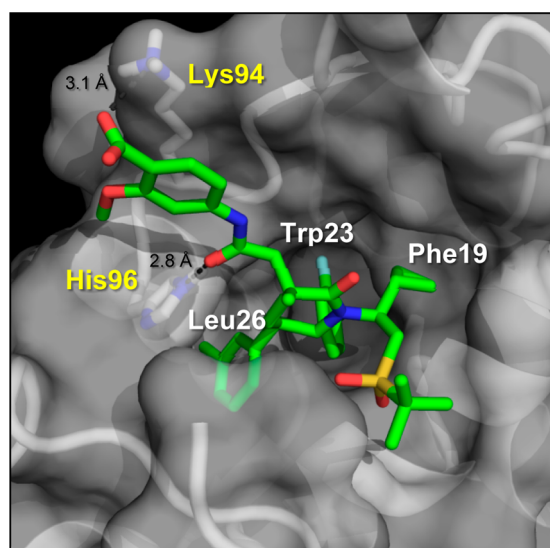


Figure 3. Cocrystal structure of **25** bound to human MDM2 (6–110) at 1.4 Å resolution (PDB code 4WT2). MDM2 binding pockets are labeled (by p53 side chain) in white. MDM2 residues Lys94 and His96 are labeled in yellow.

2.^{21,32} The amide intermediates **31a–31c** were obtained quantitatively by the ring opening of lactones **30a–30c** with (S)-2-amino-2-cyclopropylethanol. The reaction of **31a–31c** with Ts₂O and 2,6-lutidine at reflux resulted in the formation of iminium ether tosylate salts **32a–32c**.³³ Prior to installation of

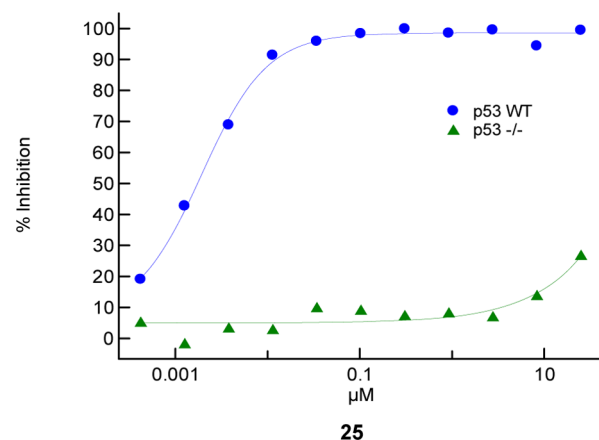


Figure 4. Cell activity of **25** is p53 dependent. In HCT-116 p53^{wt} and p53^{-/-} cells, the percentage of BrdU positive cells was measured 16 h post compound treatment by flow cytometry. The DMSO control was designated as 0% inhibition.

the *tert*-butyl sulfide group, **32a–32c** were hydrolyzed with aqueous NaHCO₃ to afford primary alcohols **33a–33c**, which were purified using silica gel column chromatography. The resulting alcohols **33a–33c** were converted again into iminium ether tosylate salts **32a–32c**, which were subjected to the nucleophilic ring opening reaction with 2-methyl-2-propane-thiol in the presence of LiHMDS. Subsequent oxidative cleavage of the allyl moiety using catalytic ruthenium tetroxide afforded carboxylic acids **2–4**.

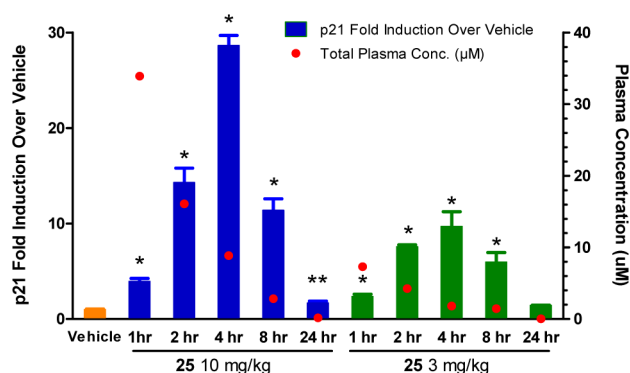


Figure 5. PD study results of compound **25** in an SJSA-1 tumor xenograft: $*p < 0.0001$; $**p = 0.01$. Female athymic nude mice were implanted subcutaneously with 5×10^6 SJSA-1 cells. When the tumors reached $\sim 250 \text{ mm}^3$, vehicle or 10 or 3 mg/kg **25** was administered orally once daily (QD) for 4 days. The mice were sacrificed at 1, 2, 4, 8, and 24 h postdose ($n = 4$ per group). The tumors were immediately removed and snap-frozen. p21 mRNA levels were measured by quantitative RT-PCR. Tumors treated with vehicle served as a negative control and indicated the baseline p21 mRNA level. Data are represented as mean p21 fold induction over vehicle, and error bars represent the SEM of data from four mice. Concentrations in blood plasma were analyzed by LC/MS/MS. The red dots denote the total plasma concentration of **25**.

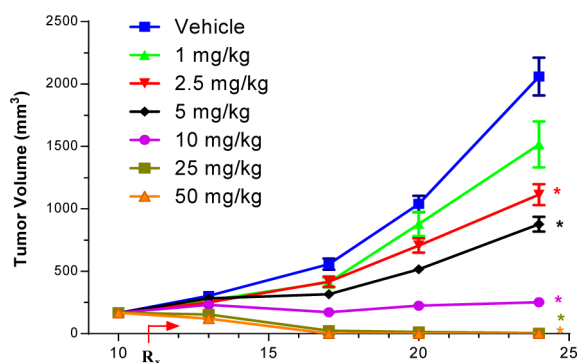


Figure 6. Treatment with **25** inhibited the growth of SJSA-1 tumors in vivo: $*p < 0.05$. SJSA-1 cells (5×10^6) were implanted subcutaneously into female athymic nude mice. Treatment with vehicle or **25** at 1, 2.5, 5, 10, 25, or 50 mg/kg QD by oral gavage began on day 11 when the tumors had reached $\sim 200 \text{ mm}^3$ ($n = 10$ per group). The tumor sizes were measured twice per week. Data represent mean tumor volumes, and error bars represent the SEM of data from 10 mice.

Finally, acids **2–4** were converted to amides **5–26** via an EDC-mediated coupling reaction, followed by the hydrolysis of ester to acid if necessary (Scheme 3).

CONCLUSION

In summary, structural modifications of **1** by (a) replacing the isopropylsulfonyl group with a *tert*-butylsulfonyl group, (b) switching the isopropyl group for a cyclopropyl group for the interaction with the Phe19_(p53) pocket in the MDM2 protein, (c) introducing an *m*-fluoro group at the C6 phenyl group, and (d) changing the carboxylic acid to a secondary amide with 4-amido-2-methoxybenzoic acid led to the discovery of **25**, the most potent and selective MDM2 inhibitor reported to date, with structural differentiation and distinct mechanisms of elimination compared to **1**. Consistent with its remarkable in

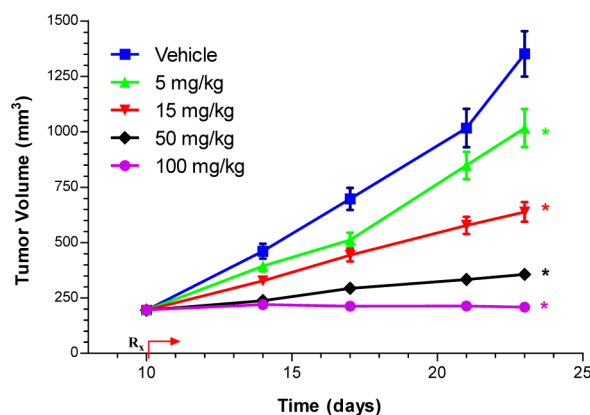


Figure 7. Inhibition of HCT-116 tumor xenograft growth by **25**: $*p < 0.005$. HCT-116 cells (2×10^6) were implanted subcutaneously into female athymic nude mice. Treatment with vehicle or **25** at 5, 15, 50, or 100 mg/kg QD by oral gavage began on day 10 when the tumors had reached $\sim 200 \text{ mm}^3$ ($n = 10$ per group). The tumor sizes and body weights were measured twice per week. Data are represented as mean tumor volumes, and error bars represent the SEM of data from 10 mice.

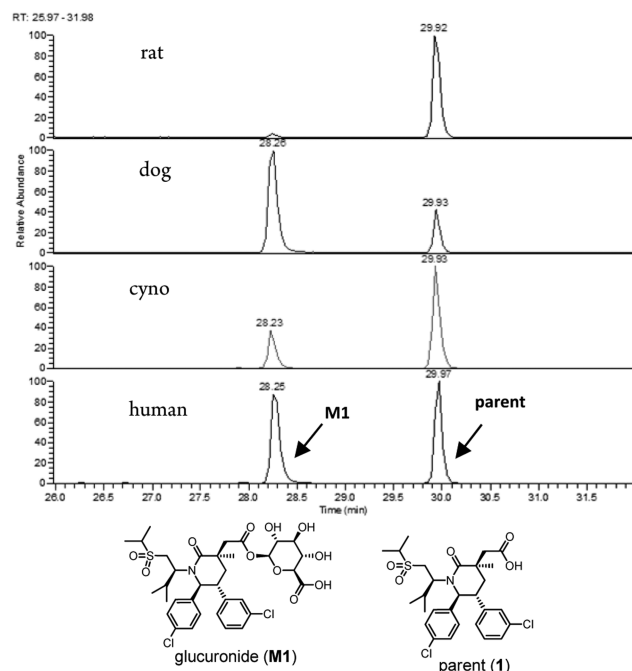
vivo antitumor activity and PK profile, **25** is a very promising candidate for the treatment of human cancer.

EXPERIMENTAL SECTION

General Chemistry. All reactions were conducted under an inert gas atmosphere (nitrogen or argon) using a Teflon-coated magnetic stir bar at the temperature indicated. Commercial reagents and anhydrous solvents were used without further purification. Analytical thin layer chromatography (TLC) and flash chromatography were performed on Merck silica gel 60 (230–400 mesh). Removal of solvents was conducted by using a rotary evaporator, and residual solvent was removed from nonvolatile compounds using a vacuum manifold maintained at approximately 1 Torr. All yields reported are isolated yields. Preparative reversed-phase high-pressure liquid chromatography (RP-HPLC) was performed using an Agilent 1100 series HPLC instrument and Phenomenex Gemini C18 column (5 μm , 100 mm \times 30 mm i.d.), eluting with a binary solvent system (A and B) using a gradient elution [solvent A, H_2O with 0.1% trifluoroacetic acid (TFA); solvent B, CH_3CN with 0.1% TFA] with UV detection at 220 nm. All final compounds were purified to $\geq 95\%$ purity as determined by the Agilent 1100 series HPLC instrument with UV detection at 220 nm using the following method: Zorbax SB-C8 column (3.5 μm , 150 mm \times 4.6 mm i.d.); mobile phase, solvent A = H_2O with 0.1% TFA, solvent B = CH_3CN with 0.1% TFA; gradient, 5–95% B (0.0–15.0 min); flow rate, 1.5 mL/min. Low-resolution mass spectrometry (MS) data were determined on an Agilent 1100 series LC/MS system with UV detection at 254 nm in low-resolution electrospray ionization (ESI) mode. High-resolution (HR) mass spectra were obtained on an Agilent 6510 Q-TOF mass spectrometer with an Agilent 1200 liquid chromatograph on the front end. ^1H NMR spectra were obtained on a Bruker Avance III 500 (500 MHz) or Bruker Avance II 400 (400 MHz) spectrometer. Chemical shifts (δ) are reported in parts per million (ppm) relative to residual undeuterated solvent as an internal reference. The following abbreviations were used to explain the multiplicities: s = singlet, d = doublet, t = triplet, q = quartet, dd = doublet of doublets, dt = doublet of triplets, m = multiplet, br = broad. Optical rotations ($[\alpha]_D$) were measured on a JASCO P-1020 polarimeter. Specific rotations are given as degrees per decimeter, and the concentrations are reported as grams per 100 mL of the specific solvent and were recorded at the temperature indicated.

1-(4-Chloro-3-fluorophenyl)-2-(3-chlorophenyl)ethanone (27b). To a solution of 4-chloro-3-fluorobenzoic acid (450 g, 2.59 mol) in MeOH (4.5 L) was added thionyl chloride (450 mL, 6.19

(a) Compound 1



(b) Compound 25

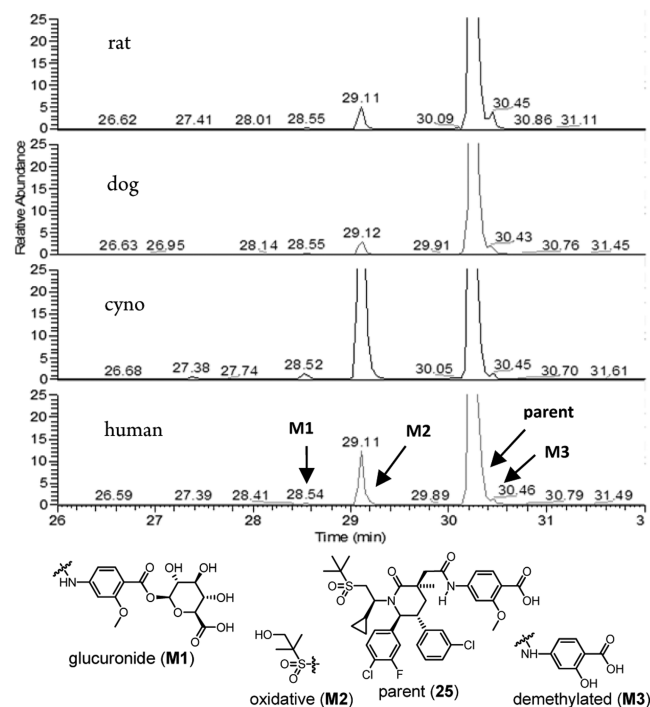
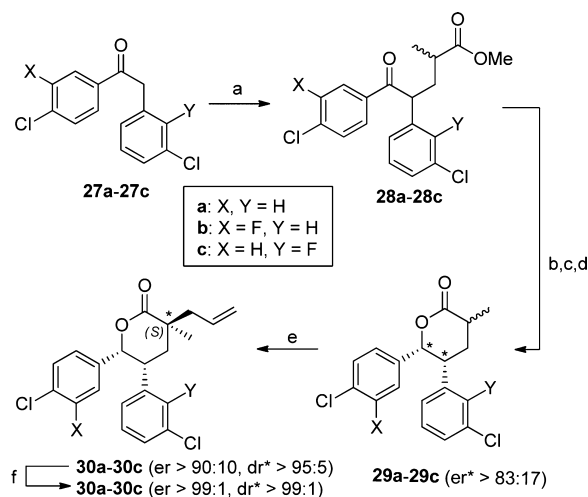
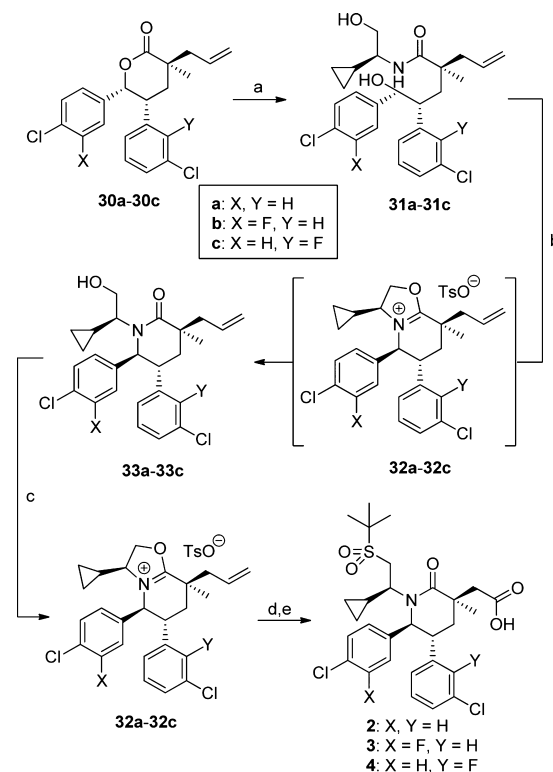


Figure 8. Representative HPLC mass chromatogram of **1** (a) and **25** (b) obtained following incubation in rat, dog, cyno, and human hepatocytes.

mol) dropwise over 30 min at 0 °C. After the mixture was stirred for 12 h at ambient temperature, the reaction was concentrated under reduced pressure, quenched (1.0 M aqueous NaHCO₃, 0.50 L), and extracted (DCM, 2 × 5.0 L). The combined organic layers were washed (brine, 2.5 L), dried (Na₂SO₄), and concentrated under reduced pressure to afford a crude methyl 4-chloro-3-fluorobenzoate

Scheme 1^a

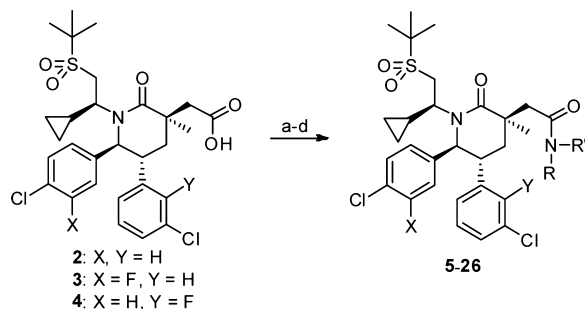
^aReagents and conditions: (a) methyl methacrylate, *t*-BuOK, THF, 74–78%; (b) RuCl₂[(*S,S*-xylBINAP)]((*S,S*-DAIPEN)], *t*-BuOK, *i*-PrOH, H₂, 50 psi, 65–75%; (c) LiOH, THF/MeOH/H₂O, 100%; (d) PPTS, toluene, reflux, 72–75%; (e) LiHMDS, allyl bromide, 69–73%; (f) recrystallization in hexanes/DCM, 88–92%.

Scheme 2^a

^aReagents and conditions: (a) (*S*)-2-amino-2-cyclopropylethanol, 100%; (b) Ts₂O, 2,6-lutidine; NaHCO₃, H₂O/DCE, 75–77%; (c) TsOH, toluene, 100%; (d) 2-methyl-2-propanethiol, LiHMDS, THF, 79–92%; (e) NaIO₄, RuCl₃, CH₃CN/EtOAc/H₂O, 80–92%.

(450 g, 93%) as a light brown solid. The crude compound was used in the next step without further purification.

To a solution of 2-(3-chlorophenyl)acetic acid (250 g, 1.47 mol) in anhydrous THF (1.8 L) was added NaHMDS (1 M in THF, 4.00 L, 4.00 mol) over 1 h at –78 °C, and the resulting mixture was stirred for another 1 h at –78 °C. Then a solution of the crude ester above (221

Scheme 3^a

^aReagents and conditions: (a) amide coupling reactions with amines for 5–26; (b) MeI, NaH, THF only for 16; (c) LiOH, MeOH/THF/H₂O for 7–12 and 14–26; (d) NH₄Cl, EDC, NaHCO₃, DMF only for 12.

g, 1.18 mol) in THF (0.50 L) was added over 1 h at -78°C . After the mixture was stirred at the same temperature for 2 h, the reaction was quenched (2 N aqueous HCl, 2.5 L) and extracted (EtOAc, 2×2.5 L). The combined organic layers were washed (brine, 2.5 L), dried (Na₂SO₄), and concentrated under reduced pressure. Flash column chromatography (SiO₂, 2% EtOAc/hexanes) provided 27b (180 g, 54%) as a white solid: ¹H NMR (400 MHz, CDCl₃) δ (ppm) 7.74 (2 H, ddd, $J = 10.1, 8.9, 1.8$ Hz), 7.56–7.48 (1 H, m), 7.26 (3 H, t, $J = 6.4$ Hz), 7.12 (1 H, d, $J = 5.7$ Hz), 4.22 (2 H, s); MS (ESI) m/z 282.9 [M + 1]⁺.

2-(3-Chloro-2-fluorophenyl)-1-(4-chlorophenyl)ethanone (27c). Compound 27c was prepared from 1-bromo-3-chloro-2-fluorobenzene and 4'-chloroacetophenone according to a procedure similar to that described for the synthesis of 27a utilizing Buchwald's ketone α -arylation conditions:³² ¹H NMR (400 MHz, CDCl₃) δ (ppm) 7.96 (2 H, d, $J = 8.5$ Hz), 7.47 (2 H, d, $J = 8.5$ Hz), 7.33 (1 H, dd, $J = 10.6, 4.3$ Hz), 7.13 (1 H, t, $J = 6.2$ Hz), 7.06 (1 H, t, $J = 7.8$ Hz), 4.31 (2 H, s); MS (ESI) m/z 282.9 [M + 1]⁺.

Methyl 4-(3-Chloro-2-fluorophenyl)-5-(4-chlorophenyl)-2-methyl-5-oxopentanoate (28b). To a solution of 27b (327 g, 1.16 mol) in THF (2.6 L) was added methyl methacrylate (136 g, 1.16 mol), followed by *t*-BuOK (1 M in THF, 115 mL, 115 mmol), at 0°C . After being stirred at 0°C for 1 h, the mixture was allowed to warm to ambient temperature and stirred for 12 h. Then the reaction was quenched (water, 1.0 L) and extracted (EtOAc, 2×2.5 L). The combined organic layers were washed (brine), dried (Na₂SO₄), and concentrated under reduced pressure. Flash column chromatography (SiO₂, 4% EtOAc/hexanes) provided 28b (1:1 mixture of two diastereomers, 330 g, 74%) as a light yellow liquid: ¹H NMR (400 MHz, CDCl₃) δ (ppm) 7.61–7.74 (4 H, m), 7.40–7.47 (2 H, m), 7.18–7.28 (6 H, m), 7.10–7.16 (2 H, m), 4.56 (2 H, m), 3.68 (3 H, s), 3.60 (3 H, s), 2.39–2.50 (2 H, m), 2.25–2.37 (2 H, m), 2.02–2.10 (1 H, m), 1.94 (1 H, ddd, $J = 13.6, 9.1, 4.2$ Hz), 1.21 (3 H, d, $J = 7.0$ Hz), 1.15 (3 H, d, $J = 7.0$ Hz); MS (ESI) m/z 383.0 [M + 1]⁺.

(5R,6R)-6-(4-Chloro-3-fluorophenyl)-5-(3-chlorophenyl)-3-methyltetrahydro-2H-pyran-2-one (29b). In a 2 L hydrogenation vessel, 28b (138 g, 360 mmol) was dissolved in 2-propanol (500 mL) and treated with *t*-BuOK (16.2 g, 144 mmol). After the mixture was stirred at 25°C for 30 min, a solution of RuCl₂[(*S,S*)-xylyBINAP][(*S,S*)-DAIPEN]] (1.76 g, 1.44 mmol) in toluene (30 mL) was added, and the resulting mixture was vigorously stirred at 25°C for 2 h. Then the vessel was purged with hydrogen five times, pressurized to 50 psi, and allowed to stir at 25°C . The reaction was recharged with additional hydrogen as needed. After 3 d, the reaction was quenched (water, 1.5 L) and extracted (EtOAc, 2×2.5 L). The combined organic layers were washed (brine, 1.5 L), dried (Na₂SO₄), and concentrated under reduced pressure. Flash column chromatography (SiO₂, 12% EtOAc/hexanes) provided (4R,5R)-isopropyl 5-(4-chloro-3-fluorophenyl)-4-(3-chlorophenyl)-5-hydroxy-2-methylpentanoate (a mixture of two diastereomers, 102 g, 69%) as a dark colored liquid: MS (ESI) m/z 435.0 [M + Na]⁺.

To a solution of the hydroxy ester above (240 g, 581 mmol) in THF (1.9 L) and methanol (0.48 L) was added LiOH (2.5 M aqueous solution, 0.48 L) at 25°C . After the mixture was stirred at 25°C for 12 h, most organic solvents were removed under reduced pressure. The residue was acidified (2 N aqueous HCl, pH ≈ 5 –6) and extracted (EtOAc, 2×1.0 L). The combined organic layers were washed (brine, 0.75 L), dried (Na₂SO₄), and concentrated under reduced pressure to give crude (4R,5R)-5-(4-chloro-3-fluorophenyl)-4-(3-chlorophenyl)-5-hydroxy-2-methylpentanoic acid (216 g, quantitatively) as a dark colored liquid, which was used in the next step without further purification.

To a solution of the hydroxy acid above (25.4 g, 68.4 mmol) in toluene (274 mL) was added pyridinium *p*-toluenesulfonate (0.516 g, 2.05 mmol). After the mixture was heated to reflux under Dean–Stark conditions for 1 h, the reaction was cooled to 25°C and concentrated under reduced pressure. The reaction was basified (saturated aqueous NaHCO₃, 150 mL) and extracted (EtOAc, 2×150 mL). The combined organic layers were washed (brine, 105 mL), dried (Na₂SO₄), and concentrated under reduced pressure. Flash column chromatography (SiO₂, 0–30% acetone/hexanes) provided 29b (a mixture of two diastereomers at C3, 18.1 g, 75%) as a pale yellow solid: MS (ESI) m/z 435.0 [M + Na]⁺.

(3S,5R,6R)-3-Allyl-6-(4-chloro-3-fluorophenyl)-5-(3-chlorophenyl)-3-methyltetrahydro-2H-pyran-2-one (30b). To a solution of 29b (18.0 g, 51.0 mmol) and 3-bromoprop-1-ene (11.0 mL, 127 mmol) in THF (100 mL) was added LiHMDS (1 M in THF, 56.1 mL, 56.1 mmol) dropwise at -40°C . The reaction was allowed to warm to -10°C and stirred at the same temperature for 3 h. Then the reaction was quenched (saturated aqueous NH₄Cl, 10 mL), diluted (water, 150 mL), and extracted (Et₂O, 2×150 mL). The combined organic layers were washed (brine, 100 mL), dried (MgSO₄), and concentrated under reduced pressure. Flash column chromatography (SiO₂, 0% to 30% acetone/hexanes) provided 30b (84% ee, 13.8 g, 69%) as a white solid.

Individual enantiomers of 30b were analyzed by analytical chiral HPLC [flow rate 1 mL/min on a Chiralcel OD-H 4.5 mm i.d. \times 250 mm, 5 μm column (Daicel Inc., Fort Lee, NJ) using 20% *i*-PrOH/hexanes as the eluent] to separate the minor enantiomer ($t_R = 5.74$ min) and the major enantiomer ($t_R = 6.73$ min). Enantiomeric excess was upgraded to >99% through recrystallization of 30b from hexanes in DCM: ¹H NMR (400 MHz, CDCl₃) δ (ppm) 7.17–7.24 (3 H, m), 6.94 (1 H, s), 6.80 (1 H, d, $J = 7.5$ Hz), 6.48 (1 H, dd, $J = 10.0, 1.9$ Hz), 6.40 (1 H, d, $J = 8.3$ Hz), 5.76–5.90 (1 H, m), 5.69 (1 H, d, $J = 5.2$ Hz), 5.13–5.20 (2 H, m), 3.81 (1 H, dd, $J = 13.9, 6.9$ Hz), 2.62 (1 H, dd, $J = 13.8, 7.6$ Hz), 2.50 (1 H, dd, $J = 13.8, 7.3$ Hz), 1.96 (2 H, d, $J = 8.4$ Hz), 1.40 (3 H, s); MS (ESI) m/z 393.1 [M + H]⁺; [α]_D²⁰ = -209 ($T = 24^{\circ}\text{C}$, $c = 1.10$, DCM); mp 96–98 $^{\circ}\text{C}$.

(3S,5R,6R)-3-Allyl-5-(3-chloro-2-fluorophenyl)-6-(4-chlorophenyl)-3-methyltetrahydro-2H-pyran-2-one (30c). Compound 30c with 80% ee was prepared as a white solid from 27c according to a procedure similar to that described for the synthesis of 30b. Individual enantiomers of 30c were analyzed by analytical chiral HPLC [flow rate 1 mL/min on a Chiralcel OD-H 4.5 mm i.d. \times 250 mm, 5 μm column (Daicel Inc., Fort Lee, NJ) using 20% *i*-PrOH/hexanes as the eluent] to separate the minor enantiomer ($t_R = 4.63$ min) and the major enantiomer ($t_R = 5.18$ min). Enantiomeric excess was upgraded to >99% through recrystallization of 30c from hexanes in DCM: ¹H NMR (400 MHz, CDCl₃) δ (ppm) 7.30 (1 H, t, $J = 7.5$ Hz), 7.16 (2 H, d, $J = 8.4$ Hz), 6.86 (1 H, t, $J = 7.8$ Hz), 6.66 (2 H, d, $J = 8.4$ Hz), 6.44 (1 H, t, $J = 6.8$ Hz), 5.78–5.89 (2 H, m), 5.13–5.22 (2 H, m), 4.16 (1 H, dd, $J = 7.3, 4.4$ Hz), 2.64 (1 H, dd, $J = 13.8, 7.5$ Hz), 2.52 (1 H, dd, $J = 13.8, 7.2$ Hz), 1.97–2.05 (1 H, m), 1.86–1.92 (1 H, m), 1.40 (3 H, s); MS (ESI) m/z 393.1 [M + H]⁺; [α]_D²⁰ = -194 ($T = 24^{\circ}\text{C}$, $c = 1.09$, DCM); mp 99–102 $^{\circ}\text{C}$.

(2S)-2-((2R)-3-(4-Chloro-3-fluorophenyl)-2-(3-chlorophenyl)-3-hydroxypropyl)-N-((S)-1-cyclopropyl-2-hydroxyethyl)-2-methylpent-4-enamide (31b). A solution of 25% sodium methoxide in methanol (60.7 mL, 265 mmol) was added to a solution of (*S*)-2-amino-2-cyclopropylethanol hydrochloride (36.5 g, 265 mmol; NetChem Inc., Ontario, Canada) in MeOH (177 mL) at 0

°C. A precipitate formed during the addition. After the addition was complete, the reaction mixture was allowed to warm to 25 °C. The reaction mixture was filtered in vacuo, and the solid phase was washed with DCM. The filtrate was concentrated under reduced pressure to provide a cloudy brown oil. The oil was taken up in DCM (150 mL) and filtered in vacuo and the solid phase washed with DCM to provide a clear orange solution. The solution was concentrated in vacuo to provide (S)-2-amino-2-cyclopropylethanol (26.7 g, 100%) as a light brown liquid.

(S)-2-Amino-2-cyclopropylethanol (26.7 g, 265 mmol) was combined with **30b** (32.0 g, 81.4 mmol), and the suspension thus obtained was heated at 100 °C overnight. The reaction mixture was cooled to 25 °C, diluted (EtOAc and 1 N aqueous HCl), and extracted (2 × EtOAc). The combined organic layers were washed (2 × 1 N aqueous HCl, 1 × water, 1 × brine), dried (MgSO₄), and concentrated under reduced pressure to provide **31b** (40.2 g, 100%) as a white solid: ¹H NMR (500 MHz, CDCl₃) δ (ppm) 7.23 (1 H, dd, *J* = 10.0, 5.0 Hz), 7.17 (1 H, m), 7.10–7.14 (2 H, m), 6.88–6.90 (2 H, m), 6.77 (1 H, dd, *J* = 8.3, 2.2 Hz), 6.01 (1 H, d, *J* = 7.1 Hz), 5.83 (1 H, m), 5.00–5.07 (2 H, m), 4.74 (1 H, d, *J* = 5.1 Hz), 3.66 (1 H, dd, *J* = 11.1, 3.1 Hz), 3.51 (1 H, dd, *J* = 11.0, 5.9 Hz), 3.08 (1 H, m), 2.97 (1 H, m), 2.39 (1 H, dd, *J* = 13.7, 7.1 Hz), 2.12 (1 H, dd, *J* = 14.4, 7.8 Hz), 2.05 (1 H, m), 1.96 (1 H, dd, *J* = 14.4, 7.8 Hz), 1.13 (3 H, s), 0.82 (1 H, dtd, *J* = 13.0, 4.9, 4.9, 3.2), 0.54 (1 H, m), 0.47 (1 H, m), 0.21–0.30 (2 H, m); MS (ESI) *m/z* 494.2 [M + H]⁺.

(3S,5R,6S)-3-Allyl-6-(4-chloro-3-fluorophenyl)-5-(3-chlorophenyl)-1-((S)-1-cyclopropyl-2-hydroxyethyl)-3-methylpiperidin-2-one (33b). To a solution of Ts₂O (66.3 g, 203 mmol) in DCM (220 mL) was added a solution of **31b** (40.2 g, 81.3 mmol) in DCM (80 mL) at 0 °C, and the reaction mixture was stirred at the same temperature for 10 min. To the reaction mixture was added 2,6-lutidine (43.6 mL, 374 mmol) dropwise at 0 °C for 10 min. The resulting solution was allowed to warm to 25 °C and then heated at reflux for 24 h. After the formation of (3S,5S,6R,8S)-8-allyl-6-(3-chloro-2-fluorophenyl)-5-(4-chlorophenyl)-3-cyclopropyl-8-methyl-2,3,5,6,7,8-hexahydrooxazolo[3,2-*a*]pyridin-4-ium 4-methylbenzenesulfonate was confirmed by LC/MS, a solution of NaHCO₃ (68.3 g, 814 mmol) in water (600 mL) and 1,2-dichloroethane (300 mL) was added to the reaction mixture successively. The reaction mixture was then heated at reflux for 1 h and cooled to 25 °C. The layers were separated, and the aqueous layer was extracted (DCM). The combined organic layers were washed (1 × 1 N aqueous HCl, 1 × water, 1 × brine) and concentrated under reduced pressure. Purification of the residue by flash column chromatography (SiO₂, 10–50% EtOAc/hexanes, a gradient elution) provided **33b** (29.8 g, 77%) as a white solid: ¹H NMR (500 MHz, CDCl₃) δ (ppm) 7.29 (1 H, t, *J* = 10.0 Hz), 7.21 (1 H, dd, *J* = 10.0, 1.6 Hz), 7.16 (1 H, dd, *J* = 10.0, 7.7 Hz), 7.02 (1 H, t, *J* = 2.0 Hz), 6.80–6.90 (2 H, m), 6.77 (1 H, dd, *J* = 7.7, 1.6 Hz), 5.87 (1 H, m), 5.16–5.19 (2 H, m), 4.86 (1 H, d, *J* = 10.0 Hz), 3.63 (1 H, dd, *J* = 11.0, 4.6 Hz), 3.36 (1 H, td, *J* = 10.3, 4.6 Hz), 3.19 (1 H, t, *J* = 10.0 Hz), 3.09 (1 H, ddd, *J* = 11.8, 9.8, 4.8 Hz), 2.57–2.65 (2 H, m), 1.85–2.20 (2 H, m), 1.25 (3 H, s), 0.85 (1 H, m), 0.57–0.67 (2 H, m), 0.26 (1 H, m), 0.06 (1 H, m); MS (ESI) *m/z* 476.2 [M + H]⁺.

(3S,5S,6R,8S)-8-Allyl-6-(3-chloro-2-fluorophenyl)-5-(4-chlorophenyl)-3-cyclopropyl-8-methyl-2,3,5,6,7,8-hexahydrooxazolo[3,2-*a*]pyridin-4-ium 4-Methylbenzenesulfonate (32b). To a solution of **33b** (73.6 g, 154 mmol) in toluene (386 mL) was added TsOH·H₂O (30.3 g, 159 mmol). The reaction was heated at reflux under Dean–Stark conditions for 4 h. Then the reaction was cooled and concentrated under reduced pressure to provide crude **32b** (97.1 g, 100%) as a pale yellow syrup. The crude product was used in the next step without further purification: ¹H NMR (500 MHz, CDCl₃) δ (ppm) 7.87 (2 H, d, *J* = 8.3 Hz), 7.25–7.32 (2 H, m), 7.16–7.20 (5 H, m), 7.08 (1 H, s), 6.80 (1 H, s, br), 5.75–5.93 (2 H, m), 5.47 (1 H, dd, *J* = 10.0, 9.1 Hz), 5.37 (1 H, d, *J* = 10.5 Hz), 5.33 (1 H, d, *J* = 17.1 Hz), 4.57–4.63 (1 H, m), 4.51 (t, *J* = 1 H, 8.6 Hz), 3.29 (1 H, m), 2.93 (1 H, t, *J* = 13.7 Hz), 2.72 (1 H, dd, *J* = 7.6 and 13.7 Hz), 2.63 (1 H, dd, *J* = 13.7, 7.3 Hz), 2.37 (3 H, s), 1.92 (1 H, dd, *J* = 13.9, 3.7 Hz), 1.57 (3 H, s), 0.33–0.50 (2 H, m), 0.08–

0.18 (1 H, m), –0.25 to –0.10 (2 H, m); MS (ESI) *m/z* 458.2 [M + H]⁺.

2-((3R,5R,6S)-1-((S)-2-(tert-Butylsulfonyl)-1-cyclopropylethyl)-6-(4-chloro-3-fluorophenyl)-5-(3-chlorophenyl)-3-methyl-2-oxopiperidin-3-yl)acetic Acid (3). 2-Methyl-2-propanethiol (15.3 mL, 135 mmol) (dried over activated 4 Å molecular sieves) was added to LiHMDS (1 M in THF, 135 mL, 135 mmol) at 25 °C under Ar, and the reaction mixture was heated to 60 °C. After 30 min, a solution of **32b** (77.6 g, 123 mmol) in THF (100 mL) was added dropwise. The reaction mixture was heated at 60 °C for 3 h and then cooled to 25 °C. The reaction mixture was quenched (water) and extracted (3 × EtOAc). The combined organic layers were washed (brine), dried (MgSO₄), and concentrated under reduced pressure to provide a yellow foam. Purification of the residue by flash column chromatography (SiO₂, 5–30% EtOAc/hexanes, a gradient elution) provided (3S,5R,6S)-3-allyl-1-((S)-2-(tert-butylthio)-1-cyclopropylethyl)-6-(4-chloro-3-fluorophenyl)-5-(3-chlorophenyl)-3-methylpiperidin-2-one (62.2 g, 92%) as an off-white foam: ¹H NMR (400 MHz, CDCl₃) δ (ppm) 7.19–7.26 (1 H, m), 7.12–7.18 (2H, m), 7.05–7.07 (1 H, m), 6.84–6.98 (1 H, m), 6.80–6.83 (1 H, m), 6.65–6.80 (1 H, m), 5.82–5.93 (1 H, m), 5.19–5.21 (1 H, m), 5.16 (1 H, s), 4.70 (1 H, d, *J* = 10.1 Hz), 3.62 (1 H, t, *J* = 11.1 Hz), 3.09 (1 H, dt, *J* = 10.4, 3.1 Hz), 2.60–2.63 (3 H, m), 2.17–2.23 (1 H, m), 2.16 (1 H, t, *J* = 13.7 Hz), 1.86 (1 H, dd, *J* = 13.5, 3.1 Hz), 1.70–1.77 (1 H, m), 1.35 (9 H, s), 1.28 (3 H, s), 0.41–0.48 (1 H, m), 0.27–0.34 (1 H, m), –0.15 to –0.09 (1 H, m), –0.89 to –0.80 (1 H, m); MS (ESI) *m/z* 548.2 [M + H]⁺.

To a rapidly stirring solution of the product above (62.2 g, 113 mmol) and NaIO₄ (24.7 g, 115 mmol) in water/EtOAc/CH₃CN (1.5:1:1, 760 mL) was added RuCl₃·H₂O (0.562 mg, 2.49 mmol) at 20 °C. The temperature quickly rose to 29 °C. The reaction mixture was cooled to 20 °C, and NaIO₄ (24.7 g, 115 mmol) was added in portions over 2 h while the internal reaction temperature was maintained below 25 °C. LC/MS 30 min after the final NaIO₄ addition indicated that the reaction was incomplete. Additional NaIO₄ (13.0 g, 60.8 mmol) was added. The temperature increased from 20 to 25 °C. LC/MS after 1.5 h indicated that the reaction was complete. The reaction mixture was filtered in vacuo, and the filter cake was washed (EtOAc). The combined filtrates were separated, and the aqueous layer was extracted (2 × EtOAc). The combined organic layers were washed (brine), dried (MgSO₄), and concentrated under reduced pressure to provide a dark green foam. Purification of the residue by flash column chromatography (SiO₂, 0–20% IPA/hexanes, a gradient elution) followed by recrystallization in 15% EtOAc/heptanes provided **3** (62.2 g, 92%) as a white solid: ¹H NMR (500 MHz, CDCl₃) δ (ppm) 7.16–7.25 (1 H, m), 7.11–7.16 (2 H, m), 7.02–7.09 (1 H, m), 6.98 (1 H, s, br), 6.88–6.90 (1 H, m), 6.75–6.87 (1 H, m), 4.98 (1 H, d, *J* = 10.8 Hz), 4.30 (1 H, t, *J* = 13.5 Hz), 3.11 (1 H, dt, *J* = 11.0, 2.7 Hz), 3.07 (1 H, d, *J* = 14.9 Hz), 2.93 (1 H, dd, *J* = 13.7, 2.0 Hz), 2.78 (1 H, d, *J* = 14.9 Hz), 2.69–2.73 (1 H, m), 2.46 (1 H, t, *J* = 13.7 Hz), 1.89–1.95 (1 H, m), 1.87 (1 H, dd, *J* = 13.7, 2.7 Hz), 1.50 (3 H, s), 1.45 (9 H, s), 0.38–0.43 (1 H, m), 0.27–0.37 (1 H, m), –0.30 to –0.22 (1 H, m), –1.10 to –1.00 (1 H, m); HRMS (ESI) *m/z* 598.1597 [M + H]⁺ (C₂₉H₃₄Cl₂FNO₅S requires 598.1592).

2-((3R,5R,6S)-1-((S)-2-(tert-Butylsulfonyl)-1-cyclopropylethyl)-5-(3-chloro-2-fluorophenyl)-6-(4-chlorophenyl)-3-methyl-2-oxopiperidin-3-yl)acetic Acid (4). Compound **4** was prepared as a white foam from **30c** according to a procedure similar to that described for the synthesis of **3** from **30b**: ¹H NMR (400 MHz, CDCl₃) δ (ppm) 7.14–7.27 (6 H, m), 6.98–7.04 (1 H, m), 5.05 (1 H, d, *J* = 10.8 Hz), 4.30 (1 H, t, *J* = 11.9 Hz), 3.65–3.75 (1 H, m), 3.16 (1 H, d, *J* = 15.7 Hz), 2.93 (1 H, d, *J* = 12.1 Hz), 2.72–2.84 (2 H, m), 2.44 (1 H, t, *J* = 13.7 Hz), 1.85 (2 H, dd, *J* = 13.7, 2.7 Hz), 1.50 (3 H, s), 1.45 (9 H, s), 0.33–0.42 (1 H, m), 0.20–0.29 (1 H, m), –0.35 to –0.26 (1 H, m), –1.15 to –1.04 (1 H, m); HRMS (ESI) *m/z* 598.1598 [M + H]⁺ (C₂₉H₃₄Cl₂FNO₅S requires 598.1592).

2-((3R,5R,6S)-1-((S)-2-(tert-Butylsulfonyl)-1-cyclopropylethyl)-5-(3-chlorophenyl)-6-(4-chlorophenyl)-3-methyl-2-oxopiperidin-3-yl)acetamide (5). Oxalyl chloride (33 μL, 0.38 mmol) was added to a solution of **2**²⁴ (200 mg, 0.344 mmol) in DCM (1.5 mL) at

25 °C. The reaction mixture was stirred at the same temperature for 1 h and then concentrated under reduced pressure to provide the acid chloride as a white foam. To a solution of the acid chloride in THF (0.5 mL) was added LiHMDS (1.0 M in THF, 0.52 mL, 0.52 mmol) at 25 °C. The reaction mixture was stirred for 6 h and was then diluted (aqueous 1 N HCl) and extracted (3 × EtOAc). The combined organic layers were washed (brine), dried (Na₂SO₄), and concentrated under reduced pressure. Purification by flash column chromatography (SiO₂, 35–100% EtOAc/hexanes, a gradient elution) provided 5 (40 mg, 20%) as an off-white foam: ¹H NMR (500 MHz, CDCl₃) δ (ppm) 7.12–7.29 (2 H, m), 7.06–7.11 (3 H, m), 7.00 (2 H, s), 6.90–6.91 (1 H, m), 6.64 (1 H, s, br), 5.63 (1 H, s, br), 4.96 (1 H, d, J = 10.8 Hz), 4.30–4.38 (m, 1 H), 3.31 (1 H, dt, J = 10.8, 2.9 Hz), 2.90–2.96 (1 H, m), 2.73–2.80 (2 H, m), 2.65–2.75 (1 H, m), 2.39 (1 H, t, J = 13.7 Hz), 2.00 (1 H, dd, J = 13.5, 2.7 Hz), 1.85–1.92 (1 H, m), 1.44 (9 H, s), 1.43 (3 H, s), 0.30–0.38 (1 H, m), 0.17–0.26 (1 H, m), –0.38 to –0.25 (1 H, m), –1.10 to –1.00 (1 H, m); HRMS (ESI) *m/z* 579.1853 [M + H]⁺ (C₂₉H₃₆Cl₂N₂O₄S requires 579.1846).

2-((3R,5R,6S)-1-((S)-2-(tert-butylsulfonyl)-1-cyclopropylethyl)-5-(3-chlorophenyl)-6-(4-chlorophenyl)-3-methyl-2-oxopiperidin-3-yl)-N-phenylacetamide (6). To a solution of 2²⁴ (119 mg, 0.204 mmol) and aniline (20 μL, 0.23 mmol) in pyridine (0.5 mL) was added EDC (117 mg, 0.612 mmol) at 0 °C. The reaction was allowed to warm to 25 °C. After the mixture was stirred for 19 h, the reaction was quenched (ice-cold 1 N aqueous HCl), extracted (2 × Et₂O), and washed (brine). The combined organic layers were dried (Na₂SO₄) and concentrated under reduced pressure. Flash chromatography (SiO₂, 15–100% EtOAc/hexanes, gradient elution) provided 6 (74 mg, 55%) as a white foam: ¹H NMR (500 MHz, CDCl₃) δ (ppm) 8.46 (1 H, s, br), 7.66 (2 H, d, J = 7.8 Hz), 7.38 (2 H, t, J = 8.3 Hz), 7.17 (1 H, t, J = 7.3 Hz), 7.02–7.09 (6 H, m), 6.99 (1 H, s), 6.86–6.89 (1 H, m), 4.94 (1 H, d, J = 10.8 Hz), 4.31 (1 H, t, J = 11.7 Hz), 3.30 (1 H, dt, J = 11.0, 2.7 Hz), 2.95 (2 H, t, J = 13.5 Hz), 2.67–2.73 (2 H, m), 2.39 (1 H, t, J = 13.7 Hz), 2.07 (1 H, dd, J = 13.7, 2.7 Hz), 1.94 (1 H, s, br), 1.47 (3 H, s), 1.45 (9 H, s), 0.30–0.40 (1 H, m), –0.28 to +0.10 (1 H, m), –0.40 to –0.28 (1 H, m), –1.32 to –1.20 (1 H, m); HRMS (ESI) *m/z* 655.2161 [M + H]⁺ (C₃₅H₄₀Cl₂N₂O₄S requires 655.2159).

4-2-((3R,5R,6S)-1-((S)-2-(tert-butylsulfonyl)-1-cyclopropylethyl)-5-(3-chlorophenyl)-6-(4-chlorophenyl)-3-methyl-2-oxopiperidin-3-yl)acetamido)benzoic Acid (7). A solution of 2²⁴ (500 mg, 0.861 mmol) and methyl 4-aminobenzoate (260 mg, 1.72 mmol) in DMF (2.5 mL) was treated with EDC (495 mg, 2.58 mmol), HOAt (352 mg, 2.58 mmol), and NaHCO₃ (217 mg, 2.58 mmol) successively at rt. After the mixture was stirred at 40 °C for 18 h, the reaction was quenched (1 N aqueous HCl), extracted (2 × EtOAc), and washed (1 × saturated aqueous NaHCO₃, 2 × brine). The combined organic layers were dried (Na₂SO₄) and concentrated under reduced pressure. Purification by RP-HPLC (45–75% A/B, gradient elution) provided methyl 4-2-((3R,5R,6S)-1-((S)-2-(tert-butylsulfonyl)-1-cyclopropylethyl)-5-(3-chlorophenyl)-6-(4-chlorophenyl)-3-methyl-2-oxopiperidin-3-yl)acetamido)benzoate (490 mg, 80%) as a white solid: MS (ESI) *m/z* 713.2 [M + H]⁺.

To a solution of the ester above (490 mg, 0.687 mmol) in THF/MeOH/H₂O (1:1:2, 20 mL) was added LiOH (2 N in H₂O, 1.03 mL, 2.06 mmol). After the mixture was stirred at 50 °C for 30 min, the reaction was quenched (ice-cold 1 N aqueous HCl), extracted (2 × EtOAc), and washed (brine). The combined organic layers were dried (Na₂SO₄) and concentrated under reduced pressure. Purification by RP-HPLC (45–65% A/B, gradient elution) provided 7 (400 mg, 83%) as a white solid: ¹H NMR (500 MHz, CDCl₃) δ (ppm) 9.47 (1 H, s, br), 8.14 (2 H, d, J = 8.8 Hz), 7.84 (2 H, d, J = 8.6 Hz), 7.02–7.23 (5 H, m), 6.85–7.02 (3 H, m), 4.98 (1 H, d, J = 10.8 Hz), 4.34 (1 H, t, J = 11.5 Hz), 3.28–3.38 (1 H, m), 2.89–3.07 (3 H, m), 2.69–2.80 (1 H, m), 2.42 (1 H, t, J = 13.7 Hz), 2.18 (1 H, dd, J = 13.7, 2.4 Hz), 1.81–1.95 (1 H, m), 1.49 (3 H, s), 1.46 (9 H, s), 0.31–0.44 (1 H, m), 0.01–0.15 (1 H, m), –0.37 to –0.25 (1 H, m), –1.26 to –1.11 (1 H, m); HRMS (ESI) *m/z* 699.2058 [M + H]⁺ (C₃₆H₄₀Cl₂N₂O₆S requires 699.2057).

Compounds 8–11, 14, 15, and 17–24. The title compounds were prepared from 2²⁴ according to a procedure similar to that described for the synthesis of 7.

Data for 4-2-((3R,5R,6S)-1-((S)-2-(tert-butylsulfonyl)-1-cyclopropylethyl)-5-(3-chlorophenyl)-6-(4-chlorophenyl)-3-methyl-2-oxopiperidin-3-yl)acetamido)2-methoxybenzoic acid (8): ¹H NMR (500 MHz, CDCl₃) δ (ppm) 9.66 (1 H, s, br), 8.14 (1 H, d, J = 8.6 Hz), 8.06–8.12 (1 H, m), 7.06–7.25 (5 H, m), 6.85–7.01 (4 H, m), 4.98 (1 H, d, J = 10.8 Hz), 4.27–4.39 (1 H, m), 4.13 (3 H, s), 3.23 (1 H, ddd, J = 13.6, 10.8, 2.7 Hz), 3.06 (1 H, d, J = 14.7 Hz), 2.96 (1 H, d, J = 12.7 Hz), 2.83 (1 H, d, J = 14.7 Hz), 2.68–2.79 (1 H, m), 2.49 (1 H, t, J = 13.6 Hz), 2.03 (1 H, dd, J = 13.6, 2.3 Hz), 1.80–1.94 (1 H, m), 1.49 (3 H, s), 1.46 (9 H, s), 0.32–0.45 (1 H, m), 0.06–0.19 (1 H, m), –0.36 to –0.24 (1 H, m), –1.21 to –1.10 (1 H, m); HRMS (ESI) *m/z* 729.2178 [M + H]⁺ (C₃₇H₄₂Cl₂N₂O₇S requires 729.2163).

Data for 4-2-((3R,5R,6S)-1-((S)-2-(tert-butylsulfonyl)-1-cyclopropylethyl)-5-(3-chlorophenyl)-6-(4-chlorophenyl)-3-methyl-2-oxopiperidin-3-yl)acetamido)3-methoxybenzoic acid (9): ¹H NMR (400 MHz, CDCl₃) δ (ppm) 8.68 (1 H, d, J = 8.4 Hz), 8.53 (1 H, s), 7.86 (1 H, dd, J = 8.5, 1.5 Hz), 7.59 (1 H, d, J = 1.8 Hz), 6.93–7.25 (7 H, m), 6.89 (1 H, td, J = 4.3, 1.6 Hz), 4.94 (1 H, d, J = 10.8 Hz), 4.35 (1 H, t, J = 11.6 Hz), 3.89 (3 H, s), 3.31–3.41 (1 H, m), 3.14 (1 H, d, J = 13.3 Hz), 2.92 (1 H, d, J = 13.1 Hz), 2.64–2.76 (2 H, m), 2.31–2.41 (1 H, m), 2.16–2.25 (1 H, m), 1.88–2.00 (1 H, m), 1.47 (3 H, s), 1.45 (9 H, s), 0.25–0.37 (1 H, m), –0.10 to +0.02 (1 H, m), –0.39 to –0.26 (1 H, m), –1.30 to –1.15 (1 H, m); HRMS (ESI) *m/z* 729.2174 [M + H]⁺ (C₃₇H₄₂Cl₂N₂O₇S requires 729.2163).

Data for 3-2-((3R,5R,6S)-1-((S)-2-(tert-butylsulfonyl)-1-cyclopropylethyl)-5-(3-chlorophenyl)-6-(4-chlorophenyl)-3-methyl-2-oxopiperidin-3-yl)acetamido)benzoic acid (10): ¹H NMR (500 MHz, CDCl₃) δ (ppm) 9.83 (1 H, s), 8.65 (1 H, dd, J = 8.2, 0.9 Hz), 8.25 (1 H, t, J = 1.7 Hz), 7.84 (1 H, d, J = 8.1 Hz), 7.43–7.49 (1 H, m), 7.15–7.35 (4 H, m), 6.91–7.15 (4 H, m), 5.01 (1 H, d, J = 10.8 Hz), 4.35 (1 H, t, J = 11.6 Hz), 3.37–3.45 (1 H, m), 3.34 (1 H, d, J = 13.0 Hz), 3.01 (1 H, d, J = 13.0 Hz), 2.98 (1 H, d, J = 13.4 Hz), 2.71–2.80 (1 H, m), 2.55 (1 H, dd, J = 13.4, 2.4 Hz), 2.31 (1 H, t, J = 13.6 Hz), 1.88–1.94 (1 H, m), 1.47 (9 H, s), 1.46 (3 H, s), 0.33–0.50 (2 H, m), 0.18–0.28 (1 H, m), –0.33 to –0.21 (1 H, m), –1.16 to –1.07 (1 H, m); HRMS (ESI) *m/z* 699.2062 [M + H]⁺ (C₃₆H₄₀Cl₂N₂O₆S requires 699.2057).

Data for 2-2-((3R,5R,6S)-1-((S)-2-(tert-butylsulfonyl)-1-cyclopropylethyl)-5-(3-chlorophenyl)-6-(4-chlorophenyl)-3-methyl-2-oxopiperidin-3-yl)acetamido)benzoic acid (11): ¹H NMR (400 MHz, CDCl₃) δ (ppm) 11.31 (1 H, s), 8.78 (1 H, d, J = 8.6 Hz), 8.12 (1 H, dd, J = 7.9, 1.5 Hz), 7.58–7.66 (1 H, m), 7.02–7.25 (6 H, m), 6.83–7.02 (3 H, m), 4.96 (1 H, d, J = 10.8 Hz), 4.31–4.45 (1 H, m), 3.34–3.46 (1 H, m), 3.17 (1 H, d, J = 13.3 Hz), 2.93 (1 H, d, J = 12.9 Hz), 2.84 (1 H, d, J = 13.5 Hz), 2.66–2.75 (1 H, m), 2.26–2.40 (2 H, m), 1.83–1.95 (1 H, m), 1.52 (3 H, s), 1.44 (9 H, s), 0.26–0.39 (1 H, m), 0.09–0.21 (1 H, m), –0.27 to –0.27 (1 H, m), –0.40 to –0.26 (1 H, m), –1.23 to –1.05 (1 H, m); HRMS (ESI) *m/z* 699.2067 [M + H]⁺ (C₃₆H₄₀Cl₂N₂O₆S requires 699.2057).

Data for 6-2-((3R,5R,6S)-1-((S)-2-(tert-butylsulfonyl)-1-cyclopropylethyl)-5-(3-chlorophenyl)-6-(4-chlorophenyl)-3-methyl-2-oxopiperidin-3-yl)acetamido)nicotinic acid (14): ¹H NMR (500 MHz, CDCl₃) δ (ppm) 12.12 (1 H, s, br), 8.89 (1 H, s, br), 8.74 (1 H, d, J = 8.6 Hz), 8.59 (1 H, d, J = 8.3 Hz), 7.15–7.42 (3 H, m), 6.85–7.14 (5 H, m), 4.96 (1 H, d, J = 10.5 Hz), 4.35 (1 H, t, J = 11.6 Hz), 3.38 (1 H, t, J = 11.5 Hz), 3.14 (1 H, d, J = 13.2 Hz), 2.97 (1 H, d, J = 13.4 Hz), 2.91 (1 H, d, J = 13.0 Hz), 2.71–2.79 (1 H, m), 2.46 (1 H, t, J = 13.6 Hz), 1.97 (1 H, d, J = 12.2 Hz), 1.80–1.91 (1 H, m), 1.57 (3 H, s), 1.44 (9 H, s), 0.28–0.37 (1 H, m), 0.17–0.27 (1 H, m), –0.39 to –0.28 (1 H, m), –1.11 to –0.96 (1 H, m); HRMS (ESI) *m/z* 700.2022 [M + H]⁺ (C₃₅H₃₉Cl₂N₃O₆S requires 700.2009).

Data for 2-4-2-((3R,5R,6S)-1-((S)-2-(tert-butylsulfonyl)-1-cyclopropylethyl)-5-(3-chlorophenyl)-6-(4-chlorophenyl)-3-methyl-2-oxopiperidin-3-yl)acetamido)phenyl)acetic acid (15): ¹H NMR (500 MHz, CDCl₃) δ (ppm) 8.78 (1 H, s, br), 7.57 (2 H, d, J = 8.3 Hz), 7.27 (2 H, d, J = 8.3 Hz), 6.76–7.20 (8 H, m), 4.95 (1 H, d, J = 10.8 Hz), 4.25–4.35 (1 H, m), 3.70 (2 H, s), 3.34 (1 H, t, J = 11.2 Hz), 2.89–3.01 (2 H, m), 2.83 (1 H, d, J = 13.7 Hz), 2.67–2.76 (1 H, m),

2.37 (1 H, t, $J = 13.6$ Hz), 2.18 (1 H, d, $J = 12.5$ Hz), 1.86 (1 H, s, br), 1.45 (3 H, s), 1.45 (9 H, s), 0.39–0.49 (1 H, m), 0.28–0.38 (1 H, m), 0.01–0.12 (1 H, m), –0.40 to –0.28 (1 H, m), –1.30 to –1.17 (1 H, m); HRMS (ESI) m/z 713.2225 $[M + H]^+$ ($C_{37}H_{42}Cl_2N_2O_6S$ requires 713.2213).

Data for (1*R*,4*r*)-4-(2-((3*R*,5*R*,6*S*)-1-((*S*)-2-(*tert*-butylsulfonyl)-1-cyclopropylethyl)-5-(3-chlorophenyl)-6-(4-chlorophenyl)-3-methyl-2-oxopiperidin-3-yl)acetamido)cyclohexanecarboxylic acid (17): 1H NMR (500 MHz, $CDCl_3$) δ (ppm) 7.14–7.36 (4 H, m), 6.83–7.13 (5 H, m), 4.96 (1 H, d, $J = 10.5$ Hz), 4.24–4.36 (1 H, m), 3.77–3.88 (1 H, m), 3.30 (1 H, t, $J = 11.7$ Hz), 2.93 (1 H, d, $J = 13.2$ Hz), 2.77–2.88 (2 H, m), 2.68–2.76 (1 H, m), 2.28–2.42 (2 H, m), 1.98–2.20 (5 H, m), 1.78–1.89 (1 H, m), 1.53–1.68 (2 H, m), 1.45 (9 H, s), 1.40 (3 H, s), 1.28–1.36 (2 H, m), 1.25–1.27 (1 H, m), 0.40–0.54 (2 H, m), 0.32–0.40 (1 H, m), 0.15–0.26 (1 H, m), –0.35 to –0.25 (1 H, m), –1.14 to –1.04 (1 H, m); HRMS (ESI) m/z 705.2530 $[M + H]^+$ ($C_{36}H_{46}Cl_2N_2O_6S$ requires 705.2526).

Data for (1*S*,4*s*)-4-(2-((3*R*,5*R*,6*S*)-1-((*S*)-2-(*tert*-butylsulfonyl)-1-cyclopropylethyl)-5-(3-chlorophenyl)-6-(4-chlorophenyl)-3-methyl-2-oxopiperidin-3-yl)acetamido)cyclohexanecarboxylic acid (18): 1H NMR (500 MHz, $CDCl_3$) δ (ppm) 7.76 (1 H, d, $J = 5.1$ Hz), 7.13–7.39 (3 H, m), 6.85–7.12 (5 H, m), 4.96 (1 H, d, $J = 10.8$ Hz), 4.29 (1 H, t, $J = 11.5$ Hz), 4.09–4.17 (1 H, m), 3.41 (1 H, td, $J = 11.3$, 4.3 Hz), 2.89–3.00 (2 H, m), 2.85 (1 H, d, $J = 13.2$ Hz), 2.67–2.76 (1 H, m), 2.47–2.57 (1 H, m), 2.20–2.35 (2 H, m), 1.97–2.06 (1 H, m), 1.85–1.96 (2 H, m), 1.67–1.84 (5 H, m), 1.45 (9 H, s), 1.40 (3 H, s), 0.39–0.52 (1 H, m), 0.30–0.39 (1 H, m), 0.14–0.23 (1 H, m), –0.38 to –0.26 (1 H, m), –1.19 to –1.07 (1 H, m); HRMS (ESI) m/z 705.2538 $[M + H]^+$ ($C_{36}H_{46}Cl_2N_2O_6S$ requires 705.2526).

Data for 4-(2-((3*R*,5*R*,6*S*)-1-((*S*)-2-(*tert*-butylsulfonyl)-1-cyclopropylethyl)-5-(3-chlorophenyl)-6-(4-chlorophenyl)-3-methyl-2-oxopiperidin-3-yl)acetamido)bicyclo[2.2.2]octane-1-carboxylic acid (19): 1H NMR (400 MHz, $CDCl_3$) δ (ppm) 7.15–7.31 (3 H, m), 6.83–7.13 (5 H, m), 6.46 (1 H, s), 4.94 (1 H, d, $J = 10.8$ Hz), 4.24–4.40 (1 H, m), 3.24–3.36 (1 H, m), 2.92 (1 H, d, $J = 13.5$ Hz), 2.58–2.80 (3 H, m), 2.32 (1 H, t, $J = 13.6$ Hz), 2.08 (1 H, dd, $J = 13.3$, 2.7 Hz), 1.89–2.04 (12 H, m), 1.77–1.87 (1 H, m), 1.44 (9 H, s), 1.36 (3 H, s), 0.30–0.43 (1 H, m), 0.14–0.27 (1 H, m), –0.40 to –0.25 (1 H, m), –1.16 to –0.98 (1 H, m); HRMS (ESI) m/z 731.2670 $[M + H]^+$ ($C_{38}H_{48}Cl_2N_2O_6S$ requires 731.2683).

Data for 1-(2-((3*R*,5*R*,6*S*)-1-((*S*)-2-(*tert*-butylsulfonyl)-1-cyclopropylethyl)-5-(3-chlorophenyl)-6-(4-chlorophenyl)-3-methyl-2-oxopiperidin-3-yl)acetyl)piperidine-4-carboxylic acid (20): 1H NMR (500 MHz, $CDCl_3$) δ (ppm) 7.13–7.28 (3 H, m), 6.83–7.13 (5 H, m), 4.94 (1 H, d, $J = 10.5$ Hz), 4.48 (1 H, t, $J = 14.1$ Hz), 4.29–4.37 (1 H, m), 4.02–4.14 (1 H, m), 3.24–3.43 (2 H, m), 2.87–3.02 (4 H, m), 2.59–2.75 (2 H, m), 2.25–2.35 (1 H, m), 2.11–2.21 (1 H, m), 2.03 (2 H, dd, $J = 13.1$, 3.1 Hz), 1.85–1.95 (1 H, m), 1.69–1.84 (2 H, m), 1.44 (9 H, s), 1.38 (3 H, d, $J = 6.6$ Hz), 0.30–0.41 (1 H, m), 0.19–0.28 (1 H, m), –0.37 to –0.25 (1 H, m), –1.13 to –1.01 (1 H, m); HRMS (ESI) m/z 691.2386 $[M + H]^+$ ($C_{33}H_{44}Cl_2N_3O_6S$ requires 691.2370).

Data for 1-(2-((3*R*,5*R*,6*S*)-1-((*S*)-2-(*tert*-butylsulfonyl)-1-cyclopropylethyl)-5-(3-chlorophenyl)-6-(4-chlorophenyl)-3-methyl-2-oxopiperidin-3-yl)acetyl)-4-methylpiperidine-4-carboxylic acid (21): 1H NMR (400 MHz, $CDCl_3$) δ (ppm) 7.14–7.27 (3 H, m), 6.83–7.12 (5 H, m), 4.94 (1 H, d, $J = 10.8$ Hz), 4.26–4.41 (2 H, m), 3.93 (1 H, t, $J = 13.5$ Hz), 3.30–3.48 (2 H, m), 2.81–3.16 (4 H, m), 2.65–2.78 (1 H, m), 2.09–2.36 (4 H, m), 1.83–1.97 (1 H, m), 1.40–1.55 (2 H, m), 1.44 (9 H, s), 1.38 (3 H, d, $J = 12.5$ Hz), 1.30 (3 H, d, $J = 3.1$ Hz), 0.29–0.40 (1 H, m), 0.17–0.28 (1 H, m), –0.39 to –0.25 (1 H, m), –1.12 to –0.99 (1 H, m); HRMS (ESI) m/z 705.2544 $[M + H]^+$ ($C_{36}H_{46}Cl_2N_2O_6S$ requires 705.2526).

Data for (1*R*,3*r*)-3-(2-((3*R*,5*R*,6*S*)-1-((*S*)-2-(*tert*-butylsulfonyl)-1-cyclopropylethyl)-5-(3-chlorophenyl)-6-(4-chlorophenyl)-3-methyl-2-oxopiperidin-3-yl)acetamido)cyclobutanecarboxylic acid (22): 1H NMR (500 MHz, $CDCl_3$) δ (ppm) 7.13–7.28 (3 H, m), 6.82–7.13 (6 H, m), 4.96 (1 H, d, $J = 10.0$ Hz), 4.63–4.76 (1 H, m), 4.22–4.35 (1 H, m), 3.24–3.35 (1 H, m), 3.13–3.22 (1 H, m), 2.94 (1 H, d, $J = 13.2$ Hz), 2.66–2.90 (5 H, m), 2.30–2.47 (3 H, m), 2.02 (1 H, d, $J = 13.2$ Hz), 1.78–1.89 (1 H, m), 1.45 (9 H, s), 1.43 (3 H, s), 0.32–0.44 (1 H, m), 0.18–0.27 (1 H, m), –0.34 to –0.23 (1 H, m), –1.16 to –1.04 (1

H, m); HRMS (ESI) m/z 677.2221 $[M + H]^+$ ($C_{34}H_{42}Cl_2N_2O_6S$ requires 677.2213).

(1*S*,3*s*)-3-(2-((3*R*,5*R*,6*S*)-1-((*S*)-2-(*tert*-butylsulfonyl)-1-cyclopropylethyl)-5-(3-chlorophenyl)-6-(4-chlorophenyl)-3-methyl-2-oxopiperidin-3-yl)acetamido)cyclobutanecarboxylic acid (23): 1H NMR (500 MHz, $CDCl_3$) δ (ppm) 8.00 (1 H, d, $J = 6.1$ Hz), 7.14–7.34 (3 H, m), 6.83–7.13 (5 H, m), 4.95 (1 H, d, $J = 10.8$ Hz), 4.52–4.62 (1 H, m), 4.26 (1 H, t, $J = 11.5$ Hz), 3.36 (1 H, t, $J = 10.8$ Hz), 2.86–3.01 (2 H, m), 2.60–2.85 (5 H, m), 2.44 (1 H, q, $J = 9.8$ Hz), 2.19–2.36 (3 H, m), 1.71–1.82 (1 H, m), 1.44 (9 H, s), 1.35 (3 H, s), 0.29–0.39 (1 H, m), 0.12–0.22 (1 H, m), –0.41 to –0.26 (1 H, m), –1.21 to –1.06 (1 H, m); HRMS (ESI) m/z 677.2229 $[M + H]^+$ ($C_{34}H_{42}Cl_2N_2O_6S$ requires 677.2213).

Data for 1-(2-((3*R*,5*R*,6*S*)-1-((*S*)-2-(*tert*-butylsulfonyl)-1-cyclopropylethyl)-5-(3-chlorophenyl)-6-(4-chlorophenyl)-3-methyl-2-oxopiperidin-3-yl)acetyl)azetidine-3-carboxylic acid (24): 1H NMR (500 MHz, $CDCl_3$) δ (ppm) 7.05–7.27 (6 H, m), 6.99 (1 H, s), 6.91 (1 H, d, $J = 3.2$ Hz), 4.95 (1 H, d, $J = 10.5$ Hz), 4.46–4.53 (2 H, m), 4.24–4.37 (3 H, m), 3.31–3.52 (2 H, m), 2.93 (1 H, d, $J = 13.0$ Hz), 2.67–2.79 (2 H, m), 2.50–2.61 (1 H, m), 2.26–2.35 (1 H, m), 2.09–2.20 (1 H, m), 1.83–1.94 (1 H, m), 1.44 (9 H, s), 1.40 (3 H, s), 0.31–0.40 (1 H, m), 0.18–0.28 (1 H, m), –0.37 to –0.26 (1 H, m), –1.12 to –1.00 (1 H, m); HRMS (ESI) m/z 663.2062 $[M + H]^+$ ($C_{33}H_{40}Cl_2N_2O_6S$ requires 663.2057).

4-(2-((3*R*,5*R*,6*S*)-1-((*S*)-2-(*tert*-butylsulfonyl)-1-cyclopropylethyl)-5-(3-chlorophenyl)-6-(4-chlorophenyl)-3-methyl-2-oxopiperidin-3-yl)acetamido)-2-methoxybenzamide (12). A solution of **8** (30 mg, 0.041 mmol) in DMF (0.3 mL) was treated with EDC (24 mg, 0.12 mmol), HOAt (17 mg, 0.12 mmol), and $NaHCO_3$ (10 mg, 0.12 mmol) successively at 25 °C. After the mixture was stirred at 40 °C for 30 min, NH_3 (7 N solution in MeOH) was added, and the resulting mixture was stirred at 40 °C for 30 min. The reaction was quenched (1 N aqueous HCl), extracted (2 \times EtOAc), and washed (1 \times saturated aqueous $NaHCO_3$, 2 \times brine). The combined organic layers were dried (Na_2SO_4) and concentrated under reduced pressure. Purification by RP-HPLC (45–65% A/B, gradient elution) provided **12** (19 mg, 63%) as a white solid: 1H NMR (500 MHz, $CDCl_3$) δ (ppm) 9.44 (1 H, s, br), 8.16 (1 H, d, $J = 8.6$ Hz), 8.02–8.16 (2 H, m), 7.03–7.29 (6 H, m), 6.78–7.03 (4 H, m), 4.97 (1 H, d, $J = 10.8$ Hz), 4.27–4.40 (1 H, m), 4.06 (3 H, s), 3.22 (1 H, ddd, $J = 13.7$, 10.9, 2.8 Hz), 2.92–3.03 (2 H, m), 2.84 (1 H, d, $J = 14.4$ Hz), 2.68–2.77 (1 H, m), 2.48 (1 H, t, $J = 13.7$ Hz), 2.00 (1 H, dd, $J = 13.6$, 2.1 Hz), 1.84–1.94 (1 H, m), 1.49 (3 H, s), 1.46 (9 H, s), 0.33–0.42 (1 H, m), 0.05–0.14 (1 H, m), –0.35 to –0.24 (1 H, m), –1.22 to –1.12 (1 H, m); HRMS (ESI) m/z 728.2325 $[M + H]^+$ ($C_{37}H_{43}Cl_2N_3O_6S$ requires 728.2322).

2-((3*R*,5*R*,6*S*)-1-((*S*)-2-(*tert*-butylsulfonyl)-1-cyclopropylethyl)-5-(3-chlorophenyl)-6-(4-chlorophenyl)-3-methyl-2-oxopiperidin-3-yl)-*N*-(4-cyanophenyl)acetamide (13). A solution of **2**²⁴ (50 mg, 0.086 mmol) and 4-aminobenzonitrile (15 mg, 0.13 mmol) in DMF (0.3 mL) was treated with EDC (50 mg, 0.26 mmol), HOAt (35 mg, 0.26 mmol), and $NaHCO_3$ (22 mg, 0.26 mmol) successively at 25 °C. After the mixture was stirred at 40 °C for 18 h, the reaction was quenched (1 N aqueous HCl), extracted (2 \times EtOAc), and washed (1 \times saturated aqueous $NaHCO_3$, 2 \times brine). The combined organic layers were dried (Na_2SO_4) and concentrated under reduced pressure. Purification by RP-HPLC (45–75% A/B, gradient elution) provided **13** (15 mg, 26%) as a white solid: 1H NMR (500 MHz, $CDCl_3$) δ (ppm) 9.60 (1 H, s, br), 7.79 (2 H, d, $J = 8.8$ Hz), 7.65 (2 H, d, $J = 8.6$ Hz), 7.05–7.24 (5 H, m), 6.81–7.02 (3 H, m), 4.97 (1 H, d, $J = 10.8$ Hz), 4.27–4.37 (1 H, m), 3.19–3.28 (1 H, m), 3.04 (1 H, d, $J = 14.7$ Hz), 2.95 (1 H, d, $J = 13.7$ Hz), 2.82 (1 H, d, $J = 14.7$ Hz), 2.68–2.78 (1 H, m), 2.49 (1 H, t, $J = 13.8$ Hz), 1.99 (1 H, dd, $J = 13.7$, 2.7 Hz), 1.80–1.93 (1 H, m), 1.49 (3 H, s), 1.45 (9 H, s), 0.34–0.40 (1 H, m), 0.02–0.10 (1 H, m), –0.35 to –0.25 (1 H, m), –1.24 to –1.14 (1 H, m); HRMS (ESI) m/z 680.2113 $[M + H]^+$ ($C_{36}H_{39}Cl_2N_3O_4S$ requires 680.2111).

4-(2-((3*R*,5*R*,6*S*)-1-((*S*)-2-(*tert*-butylsulfonyl)-1-cyclopropylethyl)-5-(3-chlorophenyl)-6-(4-chlorophenyl)-3-methyl-2-oxopiperidin-3-yl)-*N*-methylacetamido)benzoic Acid (16). To a solution of the methyl ester precursor for the synthesis of **7**, methyl

4-(2-((3*R*,5*R*,6*S*)-1-((*S*)-2-(*tert*-butylsulfonyl)-1-cyclopropylethyl)-5-(3-chlorophenyl)-6-(4-chlorophenyl)-3-methyl-2-oxopiperidin-3-yl)-acetamido)benzoate (40 mg, 0.056 mmol), in DMF (1 mL) was added NaH (60% in mineral oil, 21 mg, 0.53 mmol). After the mixture was stirred at 25 °C for 10 min, MeI (28 μL, 0.45 mmol) was added, and the mixture was stirred at 25 °C for 1 h. Then the reaction was quenched by adding water (1 mL).

To the quenched reaction above were added THF (0.5 mL), MeOH (0.5 mL), and LiOH (2 N in H₂O, 84 μL, 0.168 mmol), and the resulting mixture was stirred at 50 °C for 30 min. The reaction was quenched (ice-cold 1 N aqueous HCl), extracted (2 × EtOAc), and washed (brine). The combined organic layers were dried (Na₂SO₄) and concentrated under reduced pressure. Purification by RP-HPLC (45–65% A/B, gradient elution) provided **16** (22 mg, 56%) as an off-white solid: ¹H NMR (500 MHz, CDCl₃) δ (ppm) 8.17 (2 H, d, *J* = 8.3 Hz), 7.34 (2 H, d, *J* = 8.3 Hz), 7.05–7.25 (5 H, m), 6.80–7.03 (3 H, m), 4.86 (1 H, d, *J* = 10.5 Hz), 4.29 (1 H, t, *J* = 11.7 Hz), 3.36 (3 H, s, br), 3.24 (1 H, t, *J* = 11.2 Hz), 2.89 (1 H, d, *J* = 13.2 Hz), 2.83 (1 H, d, *J* = 14.4 Hz), 2.61–2.76 (2 H, m), 2.21–2.32 (1 H, m), 2.13–2.19 (1 H, m), 1.82–1.92 (1 H, m), 1.42 (9 H, s), 1.34 (3 H, s), 0.26–0.37 (1 H, m), 0.16–0.25 (1 H, m), –0.39 to –0.30 (1 H, m), –1.17 to –1.07 (1 H, m); HRMS (ESI) *m/z* 713.2220 [M + H]⁺ (C₃₇H₄₂Cl₂N₂O₆S requires 713.2213).

4-(2-((3*R*,5*R*,6*S*)-1-((*S*)-2-(*tert*-butylsulfonyl)-1-cyclopropylethyl)-5-(3-chloro-2-fluorophenyl)-6-(4-chlorophenyl)-3-methyl-2-oxopiperidin-3-yl)acetamido)-2-methoxybenzoic Acid (25**).** Compound **25** was prepared as a white solid from **3** according to a procedure similar to that described for the synthesis of **7**: ¹H NMR (500 MHz, DMSO-*d*₆) δ (ppm) 12.29 (1 H, s, br), 10.44 (1 H, s), 7.68 (1 H, d, *J* = 8.6 Hz), 7.54 (1 H, s, br), 7.40–7.50 (1 H, m), 7.22–7.26 (3 H, m), 7.19 (1 H, d, *J* = 8.8 Hz), 6.90–6.93 (3 H, m), 4.89 (1 H, d, *J* = 10.5 Hz), 4.05–4.20 (1 H, m), 3.77 (3 H, s), 3.40–3.50 (1 H, m), 3.02–3.16 (2 H, m), 2.66 (1 H, d, *J* = 13.7 Hz), 2.50–2.60 (1 H, m), 2.08–2.18 (2 H, m), 1.75–1.86 (1 H, m), 1.34 (9 H, s), 1.30 (3 H, s), 0.25–0.38 (1 H, m), 0.14–0.25 (1 H, m), –0.30 to –0.13 (1 H, m), –1.30 to –1.12 (1 H, m); HRMS (ESI) *m/z* 747.2063 [M + H]⁺ (C₃₇H₄₁Cl₂FN₂O₅S requires 747.2068).

4-(2-((3*R*,5*R*,6*S*)-1-((*S*)-2-(*tert*-butylsulfonyl)-1-cyclopropylethyl)-5-(3-chloro-2-fluorophenyl)-6-(4-chlorophenyl)-3-methyl-2-oxopiperidin-3-yl)acetamido)-2-methoxybenzoic Acid (26**).** Compound **26** was prepared as a white solid from **4** according to a procedure similar to that described for the synthesis of **7**: ¹H NMR (400 MHz, CDCl₃) δ (ppm) 9.50 (1 H, s, br), 8.17 (1 H, s, br), 8.13 (1 H, d, *J* = 8.4 Hz), 6.95–7.27 (7 H, m), 6.90 (1 H, d, *J* = 7.2 Hz), 5.06 (1 H, d, *J* = 11.0 Hz), 4.24–4.39 (1 H, m), 4.13 (3 H, s), 3.75 (1 H, t, *J* = 11.5 Hz), 2.84–3.09 (3 H, m), 2.68–2.80 (1 H, m), 2.46 (1 H, t, *J* = 13.7 Hz), 1.98–2.06 (1 H, m), 1.82–1.97 (1 H, m), 1.49 (3 H, s), 1.46 (9 H, s), 0.32–0.46 (1 H, m), 0.08–0.21 (1 H, m), –0.37 to –0.23 (1 H, m), –1.21 to –1.07 (1 H, m); HRMS (ESI) *m/z* 747.2085 [M + H]⁺ (C₃₇H₄₁Cl₂FN₂O₅S requires 747.2068).

■ ASSOCIATED CONTENT

● Supporting Information

In vitro biological assays, in vivo study protocols, determination of cocrystal structures of **25** with MDM2, and metabolite profiling of compounds **1** and **25** from hepatocyte incubation. This material is available free of charge via the Internet at <http://pubs.acs.org>.

Accession Codes

The coordinates of **25** with MDM2 have been deposited in the PDB with accession code 4WT2.

■ AUTHOR INFORMATION

Corresponding Author

*Phone: 650-244-2682. E-mail: yrew@amgen.com or yosuprew@yahoo.com.

Notes

The authors declare no competing financial interest.

■ ACKNOWLEDGMENTS

We thank Simon Wong for the time-dependent inhibition determinations and Manuel Ventura and Dhanashri Bagal for the acquisition of high-resolution mass spectra.

■ ABBREVIATIONS USED

BrdU, 5-bromo-2-deoxyuridine; CYP3A4, cytochrome P450 3A4; CL, clearance; DCE, 1,2-dichloroethane; DCM, dichloromethane; DKR, dynamic kinetic resolution; DMF, *N,N*-dimethylformamide; dr, diastereoselectivity ratio; EDC, *N*-(3-(dimethylamino)propyl)-*N'*-ethylcarbodiimide hydrochloride; EdU, 5-ethynyl-2'-deoxyuridine; er, enantioselectivity ratio; EtOAc, ethyl acetate; HOAt, 1-hydroxy-7-azabenzotriazole; hPXR, human pregnane X receptor; HTRF, homogeneous time-resolved fluorescence; *i*-PrOH, isopropyl alcohol; ITC, isothermal titration calorimetry; iv, intravenous; LiHMDS, lithium bis(trimethylsilyl)amide; po, per os; LiOH, lithium hydroxide; MDM2, murine double minute 2; NaH, sodium hydride; NaHMDS, sodium bis(trimethylsilyl)amide; PPTS, pyridinium *p*-toluenesulfonate; QD, once a day dosing; qRT-PCR, quantitative reverse transcription polymerase chain reaction; SAR, structure–activity relationship; SEM, standard error of the mean; SPR, surface plasmon resonance; *t*-BuOK, potassium *tert*-butoxide; TDI, time-dependent inhibition; TFA, trifluoroacetic acid; THF, tetrahydrofuran; Ts₂O, 4-toluene-sulfonic anhydride; TsOH, 4-toluenesulfonic acid

■ REFERENCES

- Vazquez, A.; Bond, E. E.; Levine, A. J.; Bond, G. L. The genetics of the p53 pathway, apoptosis and cancer therapy. *Nat. Rev. Drug Discovery* **2008**, *7*, 979–987.
- Chene, P. Inhibiting the p53-MDM2 interaction: an important target for cancer therapy. *Nat. Rev. Cancer* **2003**, *3*, 102–109.
- Vogelstein, B.; Lane, D.; Levine, A. J. Surfing the p53 network. *Nature (London, U.K.)* **2000**, *408*, 307–310.
- Kastan, M. B. Wild-type p53: tumors can't stand it. *Cell* **2007**, *128*, 837–840.
- Ventura, A.; Kirsch, D. G.; McLaughlin, M. E.; Tuveson, D. A.; Grimm, J.; Lintault, L.; Newman, J.; Reczek, E. E.; Weissleder, R.; Jacks, T. Restoration of p53 function leads to tumor regression in vivo. *Nature (London, U.K.)* **2007**, *445*, 661–665.
- Xue, W.; Zender, L.; Miething, C.; Dickins, R. A.; Hernandez, E.; Krizhanovskiy, V.; Cordon-Cardo, C.; Lowe, S. W. Senescence and tumour clearance is triggered by p53 restoration in murine liver carcinomas. *Nature (London, U.K.)* **2007**, *445*, 656–660.
- Martins, C. P.; Brown-Swigart, L.; Evan, G. I. Modeling the therapeutic efficacy of p53 restoration in tumors. *Cell* **2006**, *127*, 1323–1334.
- Oliner, J. D.; Pietenpol, J. A.; Thiagalingam, S.; Gyuris, J.; Kinzler, K. W.; Vogelstein, B. Oncoprotein MDM2 conceals the activation domain of tumor suppressor p53. *Nature (London, U.K.)* **1993**, *362*, 857–860.
- Freedman, D. A.; Levine, A. J. Nuclear export is required for degradation of endogenous p53 by MDM2 and human papillomavirus E6. *Mol. Cell. Biol.* **1998**, *18*, 7288–7293.
- Roth, J.; Dobbstein, M.; Freedman, D. A.; Shenk, T.; Levine, A. J. Nucleo-cytoplasmic shuttling of the hdm2 oncoprotein regulates the levels of the p53 protein via a pathway used by the human immunodeficiency virus rev protein. *EMBO J.* **1998**, *17*, 554–564.
- Tao, W.; Levine, A. J. Nucleocytoplasmic shuttling of oncoprotein Hdm2 is required for Hdm2-mediated degradation of p53. *Proc. Natl. Acad. Sci. U.S.A.* **1999**, *96*, 3077–3080.
- Haupt, Y.; Maya, R.; Kazanietz, A.; Oren, M. Mdm2 promotes the rapid degradation of p53. *Nature (London, U.K.)* **1997**, *387*, 296–299.

- (13) Kubbutat, M. H. G.; Vousden, K. H. Proteolytic cleavage of human p53 by calpain: a potential regulator of protein stability. *Mol. Cell. Biol.* **1997**, *17*, 460–468.
- (14) (a) Vassilev, L. T.; Vu, B. T.; Graves, B.; Carvajal, D.; Podlaski, F.; Filipovic, Z.; Kong, N.; Kammlott, U.; Lukacs, C.; Klein, C.; Fotouhi, N.; Liu, E. A. In vivo activation of the p53 pathway by small-molecule antagonists of MDM2. *Science (Washington, DC, U.S.)* **2004**, *303*, 844–848. (b) Vassilev, L. T. p53 activation by small molecules: application in oncology. *J. Med. Chem.* **2005**, *48*, 4491–4499.
- (15) (a) Ding, K.; Lu, Y.; Nikolovska-Coleska, Z.; Wang, G.; Qiu, S.; Shangary, S.; Gao, W.; Qin, D.; Stuckey, J.; Krajewski, K.; Roller, P. P.; Wang, S. Structure-based design of spiro-oxindoles as potent, specific small-molecule inhibitors of the MDM2-p53 interaction. *J. Med. Chem.* **2006**, *49*, 3432–3435. (b) Shangary, S.; Qin, D.; McEachern, D.; Liu, M.; Miller, R. S.; Qiu, S.; Nikolovska-Coleska, Z.; Ding, K.; Wang, G.; Chen, J.; Bernard, D.; Zhang, J.; Lu, Y.; Gu, Q.; Shah, R. B.; Pienta, K. J.; Ling, X.; Kang, S.; Guo, M.; Sun, Y.; Yang, D.; Wang, S. Temporal activation of p53 by a specific MDM2 inhibitor is selectively toxic to tumors and leads to complete tumor growth inhibition. *Proc. Natl. Acad. Sci. U.S.A.* **2008**, *105*, 3933–3938. (c) Yu, S.; Qin, D.; Shangary, S.; Chen, J.; Wang, G.; Ding, K.; McEachern, D.; Qiu, S.; Nikolovska-Coleska, Z.; Miller, R.; Kang, S.; Yang, D.; Wang, S. Potent and orally active small-molecule inhibitors of the MDM2-p53 interaction. *J. Med. Chem.* **2009**, *52*, 7970–7973.
- (16) Hollstein, M.; Sidransky, D.; Vogelstein, B.; Harris, C. C. p53 mutations in human cancers. *Science (Washington, DC, U.S.)* **1991**, *253*, 49–53.
- (17) Information from www.clinicaltrials.gov: (a) RG7112 (Hoffmann-La Roche), (b) RG7388 (Hoffmann-La Roche), (c) SAR405838 (Sanofi), (d) MK-8242 (Merck), (e) AMG 232 (Amgen), (f) CGM-097 (Novartis), (g) DS-3032b (Daiichi Sankyo).
- (18) Vu, B.; Wovkulich, P.; Pizzolato, G.; Lovey, A.; Ding, Q.; Jiang, N.; Liu, J.-J.; Zhao, C.; Glenn, K.; Wen, Y.; Tovar, C.; Packman, K.; Vassilev, L.; Graves, B. Discovery of RG7112: a small-molecule MDM2 inhibitor in clinical development. *ACS Med. Chem. Lett.* **2013**, *4*, 466–469.
- (19) Ding, Q.; Zhang, Z.; Liu, J.-J.; Jiang, N.; Zhang, J.; Ross, T. M.; Chu, X.-J.; Bartkovitz, D.; Podlaski, F.; Janson, C.; Tovar, C.; Filipovic, Z. M.; Higgins, B.; Glenn, K.; Packman, K.; Vassilev, L. T.; Graves, B. Discovery of RG7388, a potent and selective p53-MDM2 inhibitor in clinical development. *J. Med. Chem.* **2013**, *56*, 5979–5983.
- (20) Wang, S.; Sun, W.; Zhao, Y.; McEachern, D.; Meaux, I.; Barrière, C.; Stuckey, J.; Meagher, M.; Bai, L.; Liu, L.; Hoffman-Luca, C. G.; Lu, J.; Shangary, S.; Yu, S.; Bernard, D.; Aguilar, A.; Laurent, O. D. Stéphane Guerif, B.; Pannier P.; Gorge-Bernat, D.; Stéphanie, L. SAR405838: an optimized inhibitor of MDM2-p53 interaction that induces complete and durable tumor regression. *Cancer Res.* [Online early access]. DOI: 10.1158/0008-5472.CAN-14-0799. Published Online: Aug 21, 2014. (b) Carry, J.-C.; Garcia-Echeverria, C. Inhibitors of the p53/hdm2 protein-protein interaction-path to the clinic. *Bioorg. Med. Chem. Lett.* **2013**, *23*, 2480–2485.
- (21) (a) Rew, Y.; Sun, D. Discovery of a small molecule MDM2 Inhibitor (AMG 232) for treating cancer. *J. Med. Chem.* **2014**, *57*, 6332–6341. (b) Sun, D.; Li, Z.; Rew, Y.; Gribble, M.; Bartberger, M. D.; Beck, H. P.; Canon, J.; Chen, A.; Chen, X.; Chow, D.; Deignan, J.; Duquette, J.; Eksterowicz, J.; Fisher, B.; Fox, B. M.; Fu, J.; Gonzalez, A. Z.; Gonzalez-Lopez De Turiso, F.; Houze, J. B.; Huang, X.; Jiang, M.; Jin, L.; Kayser, F.; Liu, J.; Lo, M.-C.; Long, A. M.; Lucas, B.; McGee, L. R.; McIntosh, J.; Mihalic, J.; Oliner, J. D.; Osgood, T.; Peterson, M. L.; Roveto, P.; Saiki, A. Y.; Shaffer, P.; Toteva, M.; Wang, Y.; Wang, Y. C.; Wortman, S.; Yakowec, P.; Yan, X.; Ye, Q.; Yu, D.; Yu, M.; Zhao, X.; Zhou, J.; Zhu, J.; Olson, S. H.; Medina, J. C. Discovery of AMG 232, a potent, selective, and orally bioavailable MDM2-p53 inhibitor in clinical development. *J. Med. Chem.* **2014**, *57*, 1454–1472.
- (22) Rew, Y.; Sun, D.; Gonzalez-Lopez De Turiso, F.; Bartberger, M. D.; Beck, H. P.; Canon, J.; Chen, A.; Chow, D.; Deignan, J.; Fox, B. M.; Gustin, D.; Huang, X.; Jiang, M.; Jiao, X.; Jin, L.; Kayser, F.; Kopecky, D. J.; Li, Y.; Lo, M.-C.; Long, A. M.; Michelsen, K.; Oliner, J. D.; Osgood, T.; Ragains, M.; Saiki, A. Y.; Schneider, S.; Toteva, M.; Yakowec, P.; Yan, X.; Ye, Q.; Yu, D.; Zhao, X.; Zhou, J.; Medina, J. C.; Olson, S. H. Structure-based design of novel inhibitors of the MDM2-p53 interaction. *J. Med. Chem.* **2012**, *55*, 4936–4954.
- (23) Gonzalez-Lopez de Turiso, F.; Sun, D.; Rew, Y.; Bartberger, M. D.; Beck, H. P.; Canon, J.; Chen, A.; Chow, D.; Correll, T. L.; Huang, X.; Julian, L. D.; Kayser, F.; Lo, M.-C.; Long, A. M.; McMin, D.; Oliner, J. D.; Osgood, T.; Powers, J. P.; Saiki, A. Y.; Schneider, S.; Shaffer, P.; Xiao, S.-H.; Yakowec, P.; Yan, X.; Ye, Q.; Yu, D.; Zhao, X.; Zhou, J.; Medina, J. C.; Olson, S. H. Rational design and binding mode duality of MDM2-p53 inhibitors. *J. Med. Chem.* **2013**, *56*, 4053–4070.
- (24) Experimental details of the in vitro biological studies can be found in the Supporting Information.
- (25) Kussie, P. H.; Gorina, S.; Marechal, V.; Elenbaas, B.; Moreau, J.; Levine, A. J.; Pavletich, N. P. Structure of the MDM2 oncoprotein bound to the p53 tumor suppressor transactivation domain. *Science (Washington, DC, U.S.)* **1996**, *274*, 948–953.
- (26) Gonzalez, A. Z.; Li, Z.; Beck, H. P.; Canon, J.; Chen, A.; Chow, D.; Duquette, J.; Eksterowicz, J.; Fox, B. M.; Fu, F.; Huang, X.; Houze, J.; Jin, L.; Li, Y.; Ling, Y.; Lo, M.-C.; Long, A. M.; McGee, L. G.; McIntosh, J.; Oliner, J. D.; Osgood, T.; Rew, Y.; Saiki, A. Y.; Shaffer, P.; Wortman, S.; Yakowec, P.; Yan, X.; Ye, Q.; Yu, D.; Zhao, X.; Zhou, J.; Olson, S. H.; Sun, D.; Medina, J. C. Novel inhibitors of the MDM2-p53 interaction featuring hydrogen bond acceptors as carboxylic acid isosteres. *J. Med. Chem.* **2014**, *57*, 2963–2988.
- (27) Jordan, J. B. Unpublished results.
- (28) Experimental details of the in vivo studies can be found in the Supporting Information.
- (29) El-Deiry, W. S.; Tokino, T.; Velculescu, V. E.; Levy, D. B.; Parsons, R.; Trent, J. M.; Lin, D.; Mercer, W. E.; Kinzler, K. W.; Vogelstein, B. WAF1, a potential mediator of p53 tumor suppression. *Cell* **1993**, *75*, 817–25.
- (30) Details of the study will be reported in due course.
- (31) Experimental details of metabolite profiling from hepatocyte incubations can be found in the Supporting Information.
- (32) Lucas, B. S.; Fisher, B.; McGee, L. R.; Olson, S. H.; Medina, J. C.; Cheung, E. An expeditious synthesis of the MDM2-p53 inhibitor AM-8553. *J. Am. Chem. Soc.* **2012**, *134*, 12855–12860.
- (33) Detailed descriptions of the advantages of the iminium ether tosylate salts over the iminium ether triflate salts during the synthesis of piperidinone–sulfone series MDM2 inhibitors will be reported in a separate paper.